MATHEMATICAL MODEL FOR ESTIMATING OF SALT INTRUSION UNDER CHANGING OF CLIMATIC CONDITIONS

MR. NATTACHAT BOONCHUKUSOL

A THESIS SUBMITTED IN PARTIAL FULFILLMENT
OF THE REQUIREMENTS FOR
THE DEGREE OF MASTER OF ENGINEERING
(ENVIRONMENTAL ENGINEERING)
FACULTY OF ENGINEERING
KING MONGKUT'S UNIVERSITY OF TECHNOLOGY THONBURI
2012

Mathematical Model for Estimating of Salt Intrusion under Changing of Climatic Conditions

Mr. Nattachat Boonchukusol B.Eng. (Environmental Engineering)

A Thesis Submitted in Partial Fulfillment
of the Requirements for
the Degree of Master of Engineering (Environmental Engineering)
Faculty of Engineering
King Mongkut's University of Technology Thonburi
2012

Thesis Committee

…… Chairman of Thesis Committee
(Lect. Prapat Pongkiatkul, Ph.D.)

……. Member and Thesis Advisor
(Lect. Thidarat Bunsri, Ph.D.)

……. Member
(Asst. Prof. Cheema Soralump, Ph.D.)

Thesis Title	Mathematical Model for Estimating of Salt Intrusion under Changing of Climatic Conditions
Thesis Credits	12
Candidate	Mr. Nattachat Boonchukusol
Thesis Advisor	Dr. Thidarat Bunsri
Program	Master of Engineering
Field of Study	Environmental Engineering
Department	Environmental Engineering
Faculty	Engineering
B.E	2555

Abstract

This research aimed to predict the migration of saltwater into an unsaturated zone above an aquifer at a coastal area and mangrove forest under the change of climatic conditions. During climate change, the balance of hydrological cycle is seriously disturbed. The average daily rainfall intensity may be oscillated from 0 to 88 mmH_2O, resulting in the change of the mean sea level from 0 to 0.2 m. Catastrophic circumstances, which can occur within the year 2100, are drought occurring in relation to stagnant sea level, drought occurring in relation to sea level rise, and flood occurring in relation to stagnant sea level. The UNSAT program was employed to estimate the interface between saltwater and freshwater along the unsaturated zone for these prospective catastrophic scenarios. The UNSAT program was calibrated with a series of laboratory scale soil columns. The diameter of each column was 6.5 cm and the length of each column was 20 cm. The river sand and the silt samples with grained sizes of 0.2-0.5 mm were packed into the columns, demonstrating the sandy aquifer at the coastal area and the unsaturated zone of mangrove forest at the estuary, respectively. In the case of drought occurring in relation to stagnant sea level, the saltwater could creep to the level of 20 cm above the datum (column base) in the sand and to the 10 cm level above the silt column. As for the case of drought occurring in relation to sea level rise, the saltwater could move to the same levels as observed in the previous scenario. In the case of flood occurring in relation to stagnant sea level, the saltwater was flushed from sand column only. This indicates that the rise of sea level insignificantly affects the migration of

saltwater in the unsaturated zone. Furthermore, the capillary force of sand and silt is constant and it is much higher than the piezometric head. The flood could increase the inflow of freshwater, which caused the saltwater to be diluted and eliminated. The prediction results from UNSAT program were similar to the observation results. Then the UNSAT program was applied to the case studies: the sandy aquifer at the Thailand Gulf and the silty aquifer at the mangrove forest in Phetchaburi province, Thailand. The thicknesses of the unsaturated zones of the sandy aquifer and the silty aquifer were 5.00 and 1.50 m, respectively. In the case of drought occurring in relation to stagnant sea level, the saltwater could creep upwards to the levels of 1.50 m for the sandy aquifer and 0.25 m for the silty aquifer. As for the case of drought occurring in relation to the sea level rise, the saltwater could move upwards to the levels of 1.75 m for the sandy aquifer and 0.50 m for the silty aquifer. Furthermore, in the case of flood occurring in relation to stagnant sea level, the saltwater could be extruded downwards to the levels of 1.20 m for the sandy aquifer and 0.25 m for the silty aquifer. These findings suggest that the change of hydrological cycle can disturb the equilibrium of inflow-outflow at the aquifer rather than the fluccuating of sea level. The drought can cause the salt intrusion at the unsaturated zone. In addition, the flood can increase the infiltration of freshwater, which can either dilute or flush the saltwater from the unsaturated zone. However, the migration of saltwater in the sandy aquifer is faster than that in the silty aquifer as silt particles are finer, allowing less amount of water to permeate. This can slow down the saltwater movement when the change of climatic conditions occurs.

Keywords: Climate change/ Saltwater migration/ Mathematical model/
UNSAT program

หัวข้อวิทยานิพนธ์	แบบจำลองคณิตศาสตร์เพื่อการประเมินการรุกล้ำของน้ำทะเล ภายใต้สภาวะภูมิอากาศที่เปลี่ยนแปลง
หน่วยกิต	12
ผู้เขียน	นายณัฐชาต บุญชูกุศล
อาจารย์ที่ปรึกษา	ดร.ธิดารัตน์ บุญศรี
หลักสูตร	วิศวกรรมศาสตรมหาบัณฑิต
สาขาวิชา	วิศวกรรมสิ่งแวดล้อม
ภาควิชา	วิศวกรรมสิ่งแวดล้อม
คณะ	วิศวกรรมศาสตร์
พ.ศ.	2555

บทคัดย่อ

งานวิจัยนี้มีวัตถุประสงค์เพื่อทำนายการรุกล้ำ หรือการเคลื่อนย้ายของน้ำทะเล สู่ชั้นดินที่ไม่อิ่มตัวด้วยน้ำด้านบนของชั้นน้ำบาดาล บริเวณพื้นที่ชายฝั่งและป่าชายเลน ภายใต้สภาพภูมิอากาศที่เปลี่ยนแปลง การเปลี่ยนแปลงสภาพภูมิอากาศนั้นส่งผลรบกวนอย่างรุนแรงต่อสมดุลของวัฏจักรของน้ำ โดยที่ความเข้มฝนเฉลี่ยต่อวัน อาจแกว่งในช่วง 0 ถึง 88 มิลลิเมตรของน้ำ นำมาซึ่งการเปลี่ยนแปลงของระดับน้ำทะเลจาก 0 ถึง 0.2 เมตร วิกฤตการณ์ที่สามารถเกิดขึ้นได้ในปีคศ. 2100 ได้แก่ กรณีแห้งแล้งและระดับน้ำทะเลคงที่ กรณีแห้งแล้งและระดับน้ำทะเลเพิ่มสูงขึ้น และกรณีน้ำท่วมและระดับน้ำทะเลคงที่ทั้งนี้ใช้โปรแกรม UNSAT ในการประเมินเส้นชั้นผิวสัมผัสระหว่างน้ำเกลือและน้ำจืด ตลอดชั้นดินที่ไม่อิ่มตัวด้วยน้ำ ภายใต้วิกฤตการณ์ที่ประเมินข้างต้น ทั้งนี้ปรับแก้ค่าในโปรแกรม UNSAT ด้วยผลของชุดการทดลองคอลัมน์ระดับห้องปฏิบัติการ โดยคอลัมน์ที่ใช้ทดสอบมีเส้นผ่านศูนย์กลาง 6.5 เซนติเมตร และมีความยาว 20 เซนติเมตร โดยใช้ทรายแม่น้ำและทรายแป้งขนาดอนุภาค 0.2-0.5 มิลลิเมตรบรรจุลงในคอลัมน์ ซึ่งเป็นตัวแทนของชั้นทรายให้น้ำ ในพื้นที่ชายฝั่ง และชั้นทรายแป้งให้น้ำบริเวณป่าชายเลนปากแม่น้ำ ตามลำดับ สำหรับกรณีแห้งแล้งและระดับน้ำทะเลคงที่ น้ำเกลือสามารถเคลื่อนที่ขึ้นมาถึงระดับ 20 เซนติเมตรในชั้นทราย และ 10 เซนติเมตร ในชั้นทรายแป้ง จากด้านล่างของคอลัมน์ (ฐานคอลัมน์) ในกรณีที่แห้งแล้งและระดับน้ำทะเลเพิ่มขึ้น น้ำเกลือสามารถเคลื่อนที่ได้ในระดับใกล้เคียงกับกรณีแรก ในกรณีน้ำท่วมและระดับน้ำทะเลคงที่ น้ำเกลือถูกขับออกไปได้เฉพาะคอลัมน์ทรายเท่านั้น ซึ่งทั้งหมดชี้ให้เห็นว่า ระดับน้ำทะเลที่เพิ่มสูงขึ้นนั้นมีผลมากต่อการเคลื่อนย้ายของน้ำเกลือในชั้นที่ไม่อิ่มตัวด้วยน้ำอย่างไม่มีนัยสำคัญ นอกจากนี้ แรงคาลปิลารีของทรายและทรายแป้งมีค่าคงที่ และมีค่ามากกว่าความสูงพิโซเมตริกซ์ กรณีที่เกิดน้ำท่วมจะสามารถ

เพิ่มปริมาณการไหลเข้าของน้ำจืด ส่งผลให้น้ำเกลือถูกขับไล่และเจือจางออกไปได้จากชั้น ทั้งนี้ โปรแกรม UNSAT สามารถทำนายผลได้คล้ายคลึงกับผลการทดลอง หลังจากนั้นได้ใช้โปรแกรม UNSAT ในกรณีศึกษา บริเวณพื้นที่อ่าวไทย และบริเวณป่าชายเลนจังหวัดเพชรบุรี ประเทศไทย โดยค่าความหนาของชั้นทรายให้น้ำและชั้นทรายแป้งให้น้ำเท่ากับ 5.00 เมตร และ 1.50 เมตร ตามลำดับ ในกรณีแห้งแล้งและระดับน้ำทะเลคงที่ น้ำเกลือสามารถเคลื่อนที่ขึ้นมาได้ 1.50 เมตรในชั้นทรายให้น้ำ และ 0.25 เมตร ในชั้นทรายแป้งให้น้ำ น้ำเกลือสามารถเคลื่อนที่ขึ้นมาได้ถึง 1.75 เมตร ในชั้นทรายให้น้ำ และ 0.50 เมตรในชั้นทรายแป้งให้น้ำ ในกรณีแห้งแล้งและระดับน้ำทะเลเพิ่มขึ้น นอกจากนี้เมื่อเกิดกรณีน้ำท่วมกับระดับน้ำทะเลคงที่ น้ำเกลือสามารถเคลื่อนที่ระดับ 1.20 เมตรในชั้นทรายให้น้ำ และ 0.25 เมตรในชั้นทรายแป้งให้น้ำ ผลที่ได้ทั้งหมดนั้นทำให้ทราบได้ว่า การเปลี่ยนแปลงวัฏจักรของน้ำสามารถรบกวนความสมดุลของการไหลเข้า-ไหลออกในชั้นทรายให้น้ำมากกว่าการขึ้นลงของระดับน้ำทะเล กรณีของภัยแล้ง สามารถทำให้เกิดการรุกของน้ำทะเลเข้าสู่ชั้นดินให้น้ำ ส่วนกรณีของน้ำท่วมนั้นปริมาณน้ำจืดที่เพิ่มขึ้นจากปริมาณน้ำฝน สามารถขับไล่ หรือเจือจางน้ำเกลือในชั้นไม่อิ่มตัวด้วยน้ำ อย่างไรก็ตาม การเคลื่อนย้ายของน้ำเกลือในชั้นทรายให้น้ำนั้นเร็วกว่าชั้นทรายแป้งให้น้ำ เพราะทรายแป้งมีขนาดอนุภาคที่ละเอียดกว่า จึงมีค่าการยอมให้น้ำซึมผ่านต่ำกว่า ซึ่งทำให้ชะลอการเคลื่อนที่ของน้ำเกลือ เมื่อสภาพภูมิอากาศเปลี่ยนแปลง

คำสำคัญ: สภาพภูมิอากาศที่เปลี่ยนแปลง/ การรุกล้ำของน้ำทะเล/ แบบจำลองคณิตศาสตร์/
โปรแกรม UNSAT

ACKNOWLEDGEMENTS

The author would like to thank his advisor, Dr. Thidarat Bunsri who has always helped with the research. Also, thanks are forwarded to research committees, Dr. Prapat Pongkiatkul and Assistant Professor Dr. Cheema Soralump for their helpful and valuable comments, which significantly enhanced the quality of the work. Without their useful suggestions, the research could not be completely developed

The research facility was partially supported by the Higher Education Research Promotion and National Research University Project of Thailand, Office of the Higher Education Commission. This research is a part of Project No. EHWM-PJ-CT-12-08, which is funded by PERDO.

CONTENTS

CONTENTS (cont.)

CONTENTS (cont.)

LIST OF TABLES

LIST OF TABLES (cont.)

LIST OF FIGURES

LIST OF FIGURES (cont.)

LIST OF FIGURES (cont.)

LIST OF SYMBOLS

English symbols

a	=	Coefficient of van Genutchten's hydraulic properties model [1/cm]
D_z	=	The soil water diffusivity [cm^2/h]
g	=	Acceleration of gravity [m/s^2]
K	=	The hydraulic conductivity [cm/hr]
K_z	=	The fully saturated hydraulic conductivity [cm/hr]
k_{rw}	=	Relative permeability, [unitless]
m	=	Empirical parameters for van Genutchten model, [unitless]
p	=	Empirical parameters for van Genutchten model, [unitless]
q_z	=	Darcy's velocity in vertical direction [cm/hr]
S	=	Slope from the water retention curve of soil [unitless]
z	=	elevation [cm]

Greek symbols

θ	=	volumetric moisture content [unitless]
θ_s,	=	saturated moisture content[cm3/cm3]
θ_r	=	residual moisture content [cm3/cm3]
θp	=	center point of volumetric water content [cm3/cm3]
ψ	=	the pressure head [cm]

LIST OF ABBREVIATIONS

1D	one dimensional model
ASTM	american Society for Testing and Materials International
EC	electical conductivity
ECe	electroconductivity of soil saturated extract
EC (1:5)	electrical conductivity of a 1 to 5 soil/water suspension
g/L	gram per liter
MATLAB	MATrix LABoratory programme
mmH_2O	millimeter of water
REV	representative elementary volume
UNSAT model	Modeling of contaminants Transport in unsaturated soil

CHAPTER 1 INTRODUCTION

1.1 Statement of problems

The seawater intrusion into coastal aquifer is one of the most important environmental problems in present, which is caused by the change of climatic condition. The seawater intrusions can directly pose the impact to the sustainability of water resource in the global scale. The intrusion of seawater into groundwater aquifer is normally prevented by the ambient groundwater flux discharging towards the ocean. However, the elevation of the land near the coastal area is normally at the same or slightly lower level than the sea level. The piezometric head of groundwater may not enough to push the seawater, if the freshwater flux is low. Since the seawater entered into the aquifer, the spreading of salt into the groundwater is occurred due to the molecular diffusion. The groundwater becomes the brackish water and this can bring the serious problem into the coastal communities in several countries (U.S. Geological Survey, 2000).

Seawater intrusion is a dynamic process, which is varied seasons by seasons. However, the equilibrium between the inflow and outflow in the aquifer is controlled by the flow of groundwater. When the climate condition has been oscillated, the quantity of infiltration might be directly changed. In case of drought, the quantity of groundwater is reduced and then the salt intrusion might creep into the land with a longer distance. Another case is the quantity of groundwater is increased due to the heavy rain or storms, the high amount of groundwater and runoff can dilute the saline water at the coastal and estuaries. On the other hand, the change of climatic condition also affects to the sea level such as tide, tsunami and storm. The growth of population, the expansion of land uses for industry and agriculture, these changes can increase the salinity of groundwater at the local to regional scales (Illangasekare et al., 2006). As the prediction results from many scientific institutes, the climate change can cause either the risen of sea level and drought, or the increasing of groundwater quantity and flooding. In some areas, especially at the tropical zone may face with both. These conditions can bring either salt intrusion at the coastal area or dilution of saline water at the estuary. If the groundwater becomes brackish water, this can pose the adverse impacts to agriculture, industry, economy and society. In contrast, flood can cause the decreasing of salinity level at the

estuary and coastal area and this can disturb the mangrove and coral reef ecosystems (ICPP, 2007).

1.2 Objectives

The aim of this research is to evaluate the intrusion of seawater in coastal aquifer by using the mathematical models. The objectives are:

1. To conduct the experiment for determining the constants of hydraulic properties model.

2. To setup the laboratory scale experiments under the various conditions for calibrating to the UNSAT model that is contaminant transport under infiltration-redistribution.

3. To apply the UNSAT model, to predict the migration of salt in the vadose zones at the sandy aquifer at coastal area along the Thailand Gulf and the silty aquifer at mangrove forest, Phetchaburi, Thailand under the change of climate conditions.

1.3 Scopes

The situation of groundwater resource under climate change is relied on both sea level and quantity of recharge water. Hence the scopes of the study are:

1. The hydraulic properties equations of porous material were fitted by van Genuchten model.

- The laboratory scale soil columns were packed with sand and soil, which can represent the geoenvironmental conditions at the coastal aquifer and the mangrove forest, respectively. The sand and soil can be acknowledged as the non-reactive and reactive porous media, respectively.

2. The UNSAT model was calibrated through the laboratory scale soil columns, which were:

- The laboratory scale soil columns were prepared, by packing the porous media at the bulk density.
- The freshwater utilised in this study was the deionised water, since the deionised water could not disturb the stability of salt dissolution. The synthesis seawater was prepared

with the salinity at 35 g/L (35 permille) which was the approximate level of salinity of seawater.

- The climate change conditions assummed in this study were included three critical possible scenarios. They were drought with stationary sea level, drought with sea level rise and flood with stationary sea level.
- The tests were conducted at ambient temperature. A level of saltwater was adjusted to 0 mmH_2O above the datum (column base) for stationary sea level and 20 mmH_2O above the datum for sea level rise. The artificial infiltration was applied at the column surface at 0 cm^3H_2O/d for drought condition and 80 cm^3H_2O/d for flooding condition.

3. The UNSAT model was further applied to predict the migration of salt under the changes of climatic conditions.

- The considered area was the sandy unconfined aquifer at the Thailand Gulf and the silty aquifer at mangrove forest in Phetchaburi, Thailand.
- The initial and boundary conditions obtained from the model calibration process were input to the model.
- The real field observation reported in the history case study was introduced to verify the model.

1.4 Expected outcomes

The expected outcomes of this research are included.

1. The possible initial and boundary conditions and the kinetic rate constants for prediction the salt migration through the sandy and the silty unconfined aquifer under the climatic change condition.

2. The prediction results for salt migration under the climatic change condition in the sensitive area of sandy unconfined aquifer in the Thailand Gulf and the silty aquifer in Phetchaburi, Thailand.

1.5 Framework of research development

Figure 1.1 presents the framework of this thesis. This thesis was separated five chapters. The statement of problem is overviewed in Chapter 1. The fundamentals and historical data were critically reviewed to establish the hypothesis of research as presented in

Chapter 2. The experimental setup and the analytical procedures were described in Chapter 3. The major findings were discussed as shown in Chapter 4. The summary and further recommendation for the future was given in Chapter 5.

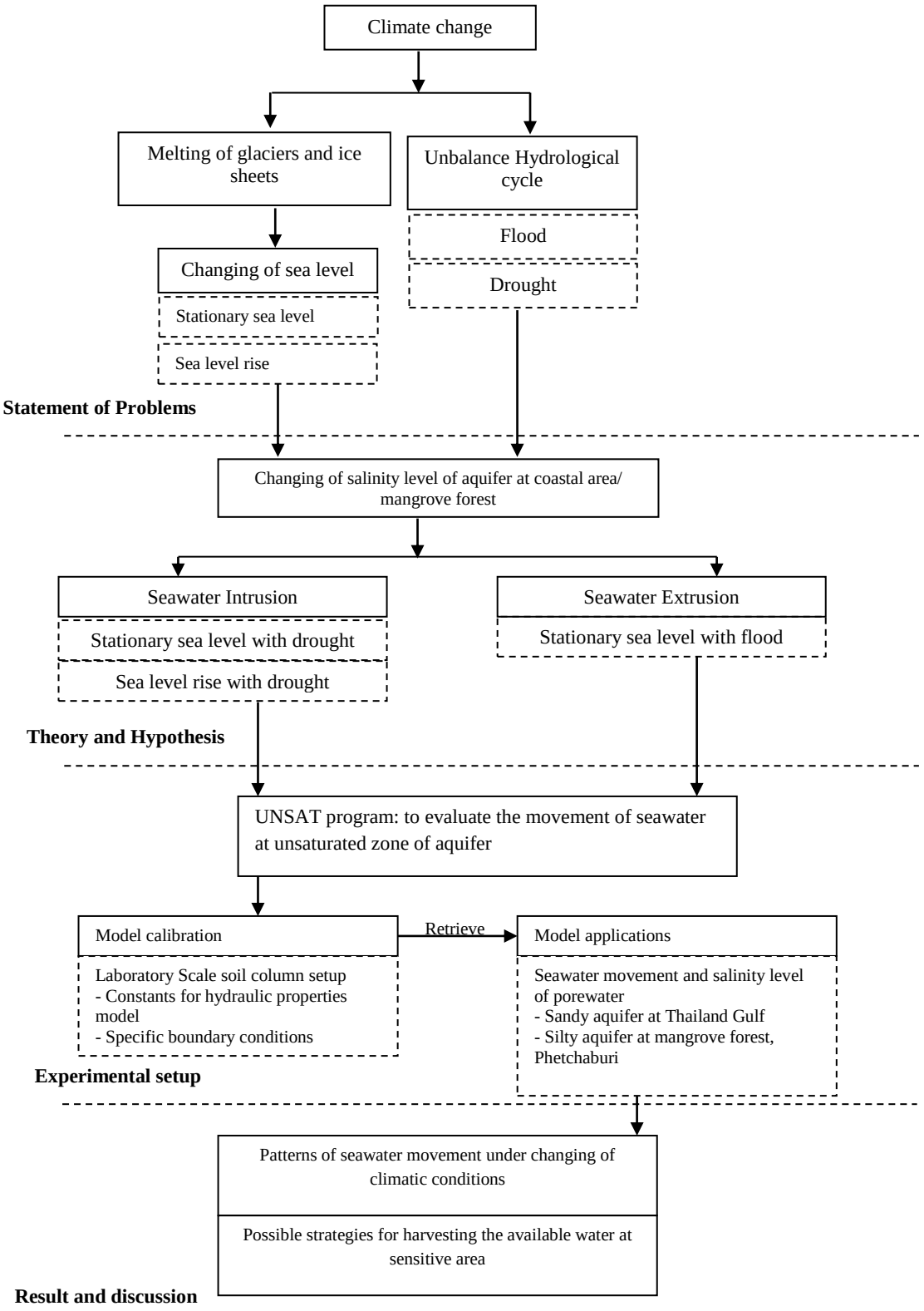

Figure 1.1 Framework of research development

CHAPTER 2 LITERATURE REVIEW

2.1 Climate change

The climate change is one of the world environmental issues, which can cause the global warming, ozone depletion, glaciation, El Niño and La Niña. The main root of climate change is the releasing of greenhouse gas to the atmosphere from the overexploitation of fossil fuel. The climate change can affect the world temperature and destroy the balance in hydrological cycle, influence the sea level rise and flood/drought. Change of climate contributes directly or indirectly affects to mankind (IPCC, 1996).

The main cause of climate change is the emission of high amounts of greenhouse gas from industrial, agricultural sectors and communities. At the UNFCCC conference, the Kyoto protocol was established to reduce the greenhouse emission to the atmosphere. The 160 countries around the world agreed to reduce the level of emission of the greenhouse gases including of carbon dioxide (CO_2), methane (CH_4), nitrous oxides (Noxs), hydro fluorocarbons, perfluorinated chemicals, sulphur hexafluoride. The agreement stated that the emission of greenhouse gases should be reducing 6-8% from the present in each year. The developed countries are accounted as the large quantity generators of greenhouse gases dealing with their industries and they should decrease greenhouse gas emission. The developing countries are classified as the small quantity generators depending on the economic condition so the reduction of greenhouse gas in the developing countries may not give any impact to relieve the climate change problem (UNFCCC conference, 1994).

The greenhouse gases are originated from both naturally and anthropologically activities. The greenhouse gas was generally emitted from natural source in the ancient period. The suitable level of greenhouse gas in the atmosphere can absorb the heat andradiation and keep the world temperature constant. Nowadays greenhouse

gas are dramatically increased by human activities especially from the burning of fossil fuel, power stations, deforestation, land use, agricultural and fertiliser, industrial process, waste disposal and treatment and transportation fuel. The high content of greenhouse gases in the atmosphere refers to the high heat storage capacity, so the

world temperature is warmer than previous. When the world temperature is increased, the hydrological cycle is shifted, which can impact to all living beings and environment (ICPP, 2007.)

2.2 Greenhouse gases

There are three major greenhouse gases, which are emitted to the atmosphere, and they can cause the climate change.

2.2.1 Carbon dioxide (CO_2)

Carbon dioxide in the atmosphere is derived from natural and human activities such as burning fuels and deforestation for habitat or agriculture. Deforestation is accounted as the main cause of the climate change as the forest can act as the sink of carbon dioxide. The trees can consume carbon dioxide in the photosynthesis process and turn carbon dioxide to carbohydrate. Besides, the photosynthesis can generate oxygen to the atmosphere. When the content of carbon dioxide in the atmosphere is increased, the high accumulation is increased too (IPCC, 2007).

2.2.2 Methane (CH_4)

Methane is originated from cultivation, fossil disintegration and biomass burning. Approximately 20% of methane gas in the atmosphere is from the fuel burning and natural burning activities. The methane gas can absorb heat 20 times higher than carbon dioxide gas (USGCRP, 2009).

2.2.3 Nitrous oxide (N_2O)

Nitrous oxide is found in the nitric acid in production, nylon fiber industry, chemical industry, plastic industry and agricultural soil. Nitrous oxide can also produce by the microbes via nitrification and denitrification process, when the nitrogen is presented. The natural sources of nitrogen are urea and ammonia. These compounds are transformed to nitrate via nitrification, an aerobic process converting ammonia-nitrogen into nitrate (NO_3). Denitrification occurs under anaerobic conditions, and involves the biological conversion of nitrate into nitrogen gas (N_2). Nitrous oxide can be an intermediate product of both these processes (USEPA, 2010).

The presence of greenhouse gases in the atmosphere can increase the world temperature. The increase of the world temperature can cause many side effects to the environment, especially shifting of hydrological cycle and sea level rise as well as salt intrusion (IPCC, 1996)

2.3 Pattern of salt intrusion on climate change

Several reports have presented the possible situations of cities along the coastal area or the cities near the estuary may take a high risk on sea level rise and salt intrusion. However, the mainland may face with flooding and drought (Adrian, 2012). The coastal area, island and estuary seem to take highly risk, when the climatic condition is rapidly changed. The salt intrusion may be observed in these sensitive areas. The salt intrusion may show the difference pattern depending on the environmental condition such as sea level rise, drought or flood (Milnes and Renard, 2003).

2.3.1 Sea level rise

When the temperature is increased, the glaciers are then melted and the volume of water in the sea is increased. Then the sea level is arisen. In the 21st century sea level had been annually increased for 0.1-0.9 m, when the world temperature was increased for 2 – 5.4 ^{o}C, respectively (IPCC, 2007). The global mean sea level (GMSL) was increased for 3.3 mm per year from 1992 to 2010 (Nicholls and Cazenave, 2010). By prediction, the global mean sea level may level up more than 1.10 – 8.80 cm in year 2100 (IPCC, 2001). The rise of sea level may affect the erosion of coastal, causing the problems in many countries and the islands which the land elevations are below the sea level. If elevation of sea level rises annually at 0.5 cm, a 5% of recharging fresh water is reduced. The salt intrusion will expand for 20% from the current situation, and 8% of land becomes the part of sea (Urbano, 2001). Approximately 12% of the salinity of water is increased from the present and the aquifer at the shore cannot be further used (Tiruneh and Motz, 2003). The seawater can move towards the land at the rate of 2.1-222 cm/day (or 0.07 to 7.4 ft/day) depending on location and tide (Paulsen et al., 2004).

Not only temperatures are arisen, but also the evaporation of seawater is increased under the climate change condition. The dissolved oxygen is decreased due to rising of seawater temperature, then the marine animals and plants are threatens. The erosion of

coastal and loss of beach is significantly observed, about 70% of the beaches around the world will be lost within 100 years (Thai Meteorological Department, 2007). The sources of water supply are contaminated by saltwater, salinity of water in the main rivers are increased (Bear et al. 1999; Masterton and Garabedian 2007; Werner and Simmons 2009).

2.3.2 Drought

The global temperature is fluctuated when the climate change phenomena is happened. Increasing of global temperature stimulates the evaporation rate of water in ocean and surface water and the melting of glaciers. The unbalance hydrological cycle can bring either flood or drought. The prediction indicates that 10-25% rainfall intensity is declined along the areas located at the equator and tropical zone (Nigel, 1999).

In case drought, the possible impacts are water shortage, increasing the water borne disease to human and animals. When water surface and groundwater are reduced in quantity, the sensitive areas, particularly the coastal area, islands and estuaries are facing with the side impacts such as soil erosion, declination of water table, salt intrusion and salty soil (Thai Meteorological Department, 2007). The impacts of salt intrusion are discussed, in particular the North Fork of Long Island, which faces the long period of drought. The salt intrusion is side effect of drought, all fresh groundwater resources in this island become saline or brackish groundwater (Misut et al., 2004). Besides, the city of Derna, Libya, which is located on the green mountain, the communities at the coast suffered from the water shortage as freshwater resource (in groundwater) is contaminated by salt due to the salt intrusion (Elhassadi, 2007). The salt intrusion can bring the seawater into the land. The seawater and freshwater can mix together and then all freshwater becomes brackish or salty water. The brackish or salty water is inconsumable by human and plants, conducting the high risk on lack of drinking water and food (Kouzana et al., 2007).

2.3.3 Flood

When global temperature is increased, it is possible to observe the flood in some areas. The evaporation rate of water is enhanced and then the storms or typhoons can be occasionally occurred in some areas. Another prediction indicates the urban, where

located near the equator and the tropical countries, may possibly face with flooding. The rainfall intensity is increased and this situation is called El Niño. In 2025, the rainfall intensity is risen 13-18% from present and the volume of runoff tends to be higher than present. The forecasting results show that the urban areas along the equator and tropical zone may be facing with flooding (Nigel, 1999).

In case of a flooding, the salt extrusion may be found, the freshwater from surface runoff or groundwater may flow downwards to the ocean. Thus, the salinity of seawater is decreased or increasing of brackish water area. When the salinity level is reduced, the ecosystems at estuaries and coral reef are affected (Nguyen et al., 2007).

2.4 Characteristics of aquifers at Thailand Gulf and Phetchaburi

The Gulf of Thailand is bordered by Cambodia, Thailand and Vietnam. The northern end of the gulf is the Bay of Bangkok at the mouth of the Chao Phraya River. The considered case study is the evaluation of salt intrusion at the coastal aquifer in the sensitive area along covers. The gulf covers roughly 320,000 km². The depth of seawater at Gulf of Thailand is relatively shallow with a averaged depth is 45 m, and the maximum depth only 80 m. The unsaturated zone is 5-12 m deep and the aquifer is sandy aquifer. An enormous amount of freshwater inflow from the rivers, such as the Chao Phraya, the Mae Klong and the Bang Pakong are filled to the Thailand Gulf. Besides, these main rivers also carry a high amount of sediment, forming the delta. The freshwater can flow slowly at estuary and delta along the gulf. The salinity of seawater at Thailand Gulf is constant at 30-32.5 permille. Only at the greater depths does water with a higher salinity 35 permille. However, the advection brings the highly salinity seawater flow through the South China sea, which 50 m deeper than the Thailand Gulf (Department of marine and coastal resource).

Phetchaburi is another considered location, enriching of mangrove forest. Phetchaburi is at the northern end of the Malay Peninsula, connected with Thailand Gulf. The mangrove forest covers the total area of 199 km². The mean depth of sea level at the shore is 10 m, and the maximum depth is only 50 m. Since the mangrove root can retard the flow of freshwater towards the sea, the sediments can be rapidly deposited along the forest. The deposited seiment could increase the thickness of aquifer. The unsaturated zone is currently at 0.5-1 m deep. The aquifer is classified as silty aquifer. The salinity

of water at the mangrove forest is slightly lower than the seawater, the brackish water always accumulated in the mangrove forest (NOAA, 1990) Even though the degree of serious of environmental issues derived from climate change is unpredictable, salt intrusion is always concerned as the frontier of the problems. The salt intrusion seemed to be the classic issue of a density-dependent problem in groundwater hydrology, the density-dependent groundwater flow, hydraulic head, salt distribution, and salt seepage. The salt intrusion can definitely increase salt load in aquifer and finally harm to the ecological systems (Giambastiani et al. 2007).

2.5 Effects of salinity to availibilty of groundwater source

The salinity of the water is presented the level of soluble salts containing in water. For the seawater, the salinity normally indicates the concentration of chloride. The relationship between salinity and chloride is defined as follows (Dittmar, 1884).

$$S(‰) = 0.03 + 1.80655\ Cl\ (‰) \quad (2.1)$$

The salinity is measured in parts per thousand, permille and the symbol of ‰ is presented the unit of parts per thousand. The constant 0.03 is negligible, so the relation can be simplified as follows.

$$S(‰) = 1.80655\ Cl\ (‰) \quad (2.2)$$

The salinity can be indirectly measured using the conductivity meter. The temperature and pressure adjusting factors are served to correct the measuring conductivity. This measurement can be called the practical measurement of salinity, which determines the proportion of electrical conductivity towards the concentration of chloride ions. If the concentration of chloride ions increase, the electrical conductivity is also increased (Demirel, 2003).

The water salinity level is useful to classify the water quality. If the salinity level is less than 0.21 permille, this is classified as the freshwater. The salinity at range of 0.21-30 permille is accounted as brackish water. When the salinity is higher than 30 permille, this is seawater (Garrison, 2007). The water from different sources has presented the

different levels of salinity. The seawater salinity is normally at 35 permille, however the brackish water in the coastal areas and estuaries may present the different salinity level seasons by seasons. The highly oscillated of salinity and increase of sea level, together with different amounts of recharged water from flood and drought can highly affect the salinity level in groundwater. The salinity can be increased and decreases rapidly under the changes of environmental conditions. Whenever water is contaminated with salt, the directly and indirectly impacts can disturb all living beings. The impacts are included (Cynthia, 2009).

- The increase and decrease of salinity in the groundwater and seawater can directly affect the marine ecosystem, coastal and fishery. The propagation and growth of fish can be disturbed, resulting in number and diversity of aquatic animals or plant are greatly reduced and extinct.
- Excessive salts in the root zone can decrease the osmotic pressure. The plants cannot obtain the water and plants are under stress or lack of water dealing with osmotic stress. As soon as the soil salinity increases, the plants may difficultly extract water from soil pores. The excessive sodium and chloride are the ionic toxic to plants, the leaf burn and defoliation may be occurred and eventually dead. The ionic imbalance of salts can reduce the ability of plants to take the nutrients (Hanson, 1999).
- As soon as soil becomes highly saline soil, its physical properties are dramatically changed. The fine particles of silts and clays can bind together, conducting highly dense soil. The increases of soil salinity can aggregate and increase soil stability (Rhoades, 1977).
- Salt intrusion can indirectly affect the agricultures and then a shortage of food may be faced. If the salty water is consumed, the human may suffer with renal disease, hypertension and cardiovascular disease. The kidney can be finally attacked (The United States Renal Data System, USRDS, 2012).
- The coastal collapse, highly saline in soil, brackish or salty groundwater other effects cause lose of land uses, so too society and economic may be declined.

The salinity of water can be directly detected, but the soil salinity can be indirectly measured by the specific electrical conductivity (EC) of a soil supernatant solution. The ratio of soil to water was controlled at 1 to 5, which was called EC (1:5). A 20 g of soil specimen were mixed with 100 g of deionised water prior to measuring the EC (1:5). A

saturated extract (ECe) was introduced to convert the value of EC(1:5) to the value of specific electrical conductivity of soil matrix. The calculation was formulated as follow (Shaw, 1999).

$$EC_e = f \times EC(1:5) \tag{2.3}$$

where f is the multiplication factor based on soil texture. For sand and slit, the values of f are 12.5 and 6.0 respectively.

The salt intrusion is correlated to the movement of sodium chloride through the soil pore. The measurement of salinity of soil porewater can be done by the electrical conductivity measurement, however, the advection-dispersion of saltwater along the soilpore cannot be measured. The mathematical model is employed to estimate the transport of saltwater through the soilpore, which is the unsaturated zone. The governing equations are mathematically derived to describe the transport of salt into the soil pore as follows.

2.6 Mathematical model developement

The migration of salt into aquifer can be separated into two cases, depending on the mixing process between seawater and groundwater. A sharp interface model assumes no mixing between salt water and fresh water and a dispersive interface model assumes a transition zone between the two fluids where mixing occurs under dispersion (Adrian, 2009). The sharp interface is influenced by the fiction of seawater and freshwater and miscible fluid is obtained in the mixing zone. Baden-Ghyben (1889) and Herzberg (1901) had modeled the static equilibrium and a hydrostatic pressure distribution in the freshwater with stationary sea level (cited in Cliffs, 1979). The seawater density is normally at 1.025 g/cm^3 and freshwater density is at 1.0 g/cm^3. The seawater may be observed underneath the freshwater. It height hydraulic pressure head of saltwater is 40 times higher than the freshwater.

According to the U-tube test on coastal predicament, a hydrodynamic force always exceeds hydrostatic force. An energy balance is maintained as freshwater is flowing on the layer of seawater, even there is no mixing. A horizontal interface may expand by

freshwater floating above saltwater. Badon Ghyben Herzberg approximating model had been defaulted the vertical head gradient because inexact near the coast. The equation for groundwater discharge to seawater and freshwater interface can be described by Darcy's equation (Custodio, 1987; Falkland, 1991).

The area of aquifer containing the sea wedge can be assumed as the fixed head system, which can be normally observed at the coast (Custodio, 1987). Hence, the position of the toe at the seawater wedge is situated at the intersection of seawater and freshwater interface. The seawater intrusion can determined through integration of a steady-state mass balance and Darcy's law. Bear and Dagan (1964) presented that the Badon Ghyben Herzberg approximation horizontal flow assumption can be combined to provide a relation between the length of the sea water intrusion and the discharge to the sea.

An important effect of the transition zone which seaward flow is the transport of saltwater to the sea, from continuity saltwater must exits a small landward flow in the seawater region. For example field measurement and experimental studies have insisted the land exit flow movement of the salt water. Predominant mixing mechanism is acted by tidal, fluctuations of groundwater. The thicknesses of transition zone become largest near the shoreline.

The governing equations for salt movement in unsaturated zone can be separated into two parts, which are the water movement and salt transport. The water movement in the unsaturated zone is relied on the advection and dispersion process. However, the conditions assigned in this research are dealt with the drought and heavy rainfall (flood), hence the unsaturated zone may be acted as infiltration-redistribution system. The infiltration-redistribution systems can fill the freshwater into soil pore and abstract seawater upwards.

2.6.1 Richard's equation

Infiltration is assumed water move under gravitational force and the movement of water passes the effective soil pores can be simplified that water moves only in liquid state.

Without impact of airflow in soil, Richards equation (Richards, 1931) could be traditionally described the 1D vertical unsaturated flow in a porous media as follows.

$$\frac{\partial}{\partial z}\left[K_z k_{rw}\left(\frac{\partial \psi}{\partial z}+1\right)\right]=S\frac{\partial \psi}{\partial t} \tag{2.4}$$

where k_{rw} is the relative hydraulic conductivity [unitless], K_z is the fully saturated hydraulic conductivity [L T^{-1}], S is the specific moisture capacity, z is the elevation head [L], t is the time interval [T] and ψ is the pressure head [L].

As the soil pores are connected, the continuity flow always occurs. Darcy's velocity is described the flow of infiltration and redistribution along the unsaturated zone. The equation can be written as follows (Huyakorn et al., 1984).

$$q_z=-K_z k_{rw}\left(\frac{\partial[\psi+z]}{\partial z}\right) \tag{2.5}$$

where q_z is Darcy's velocity in vertical direction [L T^{-1}].

Another way to describe the movement of water is determining the soil volumetric moisture content. When the soil pore is filled with water, the volumetric moisture content is increased. The relationship between pressure head and volumetric moisture content is defined as the hydraulic properties model.

2.6.2 Soil hydraulic properties equation

The flow of groundwater could consider volumetric water content in soil and changing pressure head in pore soil water which this equation will present relationship between pressure head with volumetric water content. And this equation could change parameter to another parameter. The hydraulic properties equations used in this research is model derived by van Genuchten (1980).

van Genuchten (1980) derived the hydraulic properties equations based on the equation of Brooks and Coley (1964). The hydraulic properties equations are presented as follows.

$$\theta = \theta_r + \frac{\theta_s - \theta_r}{(1 + (a|\psi|^p)^m} \tag{2.6}$$

where a is the soil water retention function [L^{-1}], m and p are the empirical parameters yielded from the hydraulic properties curve [unitless], respectively.

The relative hydraulic permeability can be defined as follows.

$$k_{rw} = \frac{\left\{1 - (a|\psi|)^{p-1}\left[1 + (a|\psi|)\,p\right]^{-m}\right\}^2}{[1 + (a|\psi|)^p]^{m/2}} \tag{2.7}$$

An example of water retention curve fitted by VG is presented in Figure 2.1

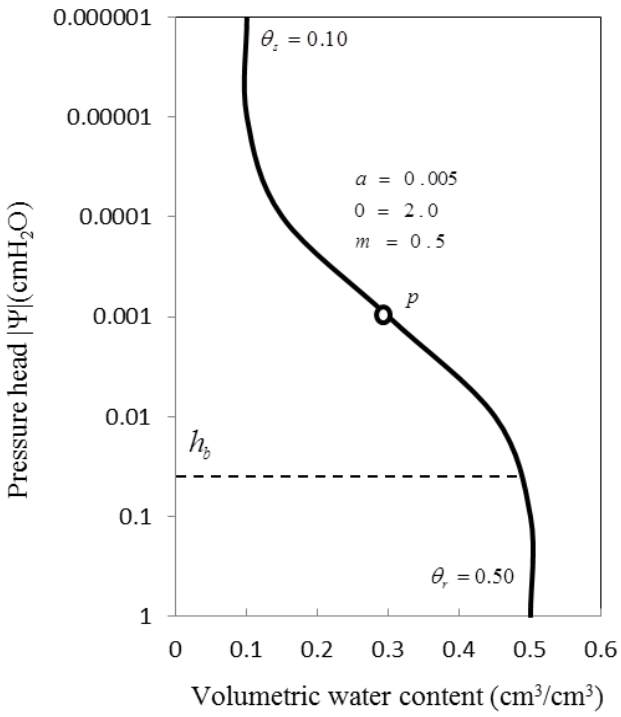

Figure 2.1 Water retention curve

The constant values for the coefficients presented in VG equations were given in Table 2.1. The coefficients were sorted by soil textures in accordance with USDA textural classes (U.S. Department of Agriculture, 2001) (Carsel et al., 1988).

Table 2.1 Constant empirical coefficients for VG equations (Carsel et al., 1988)

Soil Type	Saturated Moisture Content, θ_s	Residual Moisture Content, θ_r	a (cm^{-1})	p
Clay*	0.38	0.068	0.008	1.09
Clay loam	0.41	0.095	0.019	1.31
Loam	0.43	0.078	0.036	1.56
Loam sand	0.41	0.057	0.124	2.28
Silt	0.46	0.034	0.106	1.37
Silt loam	0.45	0.067	0.020	1.41
Silty clay	0.36	0.070	0.005	1.09
Sity clay loam	0.43	0.089	0.010	1.23
Sand	0.43	0.045	0.145	2.68
Sandy clay	0.38	0.100	0.027	1.23
Sandy clay loam	0.39	0.100	0.059	1.48
Sandy loam	0.41	0.065	0.075	1.89

Note: *Agricultural soil, less than 60% clay.

2.6.3 Salt transport

The approximate mass of saltwater in the soil pore at the unsaturated zone is traditionally determined by the mass balance concept. The mass balance equation can be simplied as follows (Bunsri, 2006).

Rate of accumulation = Rate of input – Rate of output ±Rate of reaction (2.8)

Considering the salt movement in unsaturated zone, the advection and dispersion processes can bring saltwater far away from source. The mass balance equation for salt transport is unsaturated soil is presented as follows (Bunsri, 2006).

$$\frac{\partial}{\partial z}\left(D_z \frac{\partial C}{\partial z}\right) - q_z \frac{\partial C}{\partial z} = \theta\kappa\left[\frac{\partial C}{\partial t} + \lambda C\right] \tag{2.9}$$

where C is the concentration of contaminant [M L^{-3}], D_z is the dispersion coefficient [L^2 T^{-1}] θ is the volumetric moisture content [L^3 L^{-3}] and κ is the retardation factor;

$\left(\kappa = 1 + \frac{\rho_B K_d}{\theta}\right)$[unitless]. ρ_B is the bulk density of soil [M L^{-3}], K_d is the distribution coefficient [L^{-3} M] and λ is the biodecay factor [T^{-1}].

The terms presented in the equation are involving dispersion, advection, accumulation and biodegradation, respectively. Salt is accounted as the non reactive constituent. Hence the term λ becomes 0.0 and κ is constant at 1.00 (Bunsri, 2006).

Applying Galerkin's finite element method, Richards' equation (Equation 2.4) and mass balance equation (Equation 2.9), the approximate solutions are obtained as follows (Bunsri, 2006).

Richards' Equation:

$$\left[A_{ij}\right]\psi_j + \left[B_{ij}\right]\frac{\partial \psi_j}{\partial t} = \{E_i\} \tag{2.10}$$

where ψ_j is the nodal pressure head [L]. N_i and N_j present the nodal function, M_C is the specific moisture capacity; $M_C = \frac{-a^p(p-1)(\theta_s - \theta_r)|\psi|^{p-1}}{\left[1+(a|\psi|)^p\right]^{m+1}}$. θ_s and θ_r are the saturated and residual moisture content, respectively, [L^3 L^{-3}]. The matrices are defined as follows.

$$\left[A_{ij}\right] = \sum_e \int_{z=0}^{z=L} K_z k_{rw}\left(\frac{\partial N_i}{\partial z}\frac{\partial N_j}{\partial z}\right)dz;$$

$$\left[B_{ij}\right] = \sum_e \int_{z=0}^{z=L} N_i N_j M_C dz; \qquad \textit{and}$$

$$\{E_i\} = N_i K_z k_{rw}\left(\frac{\partial \psi}{\partial z} + 1\right)\Bigg|_{z=0}^{z=L} - \sum_e \int_{z=0}^{z=L} K_z k_{rw}\frac{\partial N_i}{\partial z}dz$$

Mass balance equation:

$$\left(\left[P_{ij}\right] + \left[R_{ij}\right]\right)C_j + \left[Q_{ij}\right]\frac{\partial C_j}{\partial t} = \{S_i\} \tag{2.11}$$

where C_j is the nodal concentration of contaminant [M L^{-3}]. The matrices are defined as follows.

$$\left[P_{ij}\right]=\sum_{e}\int_{z=0}^{z=L}\left(D_z\frac{\partial N_i}{\partial z}\frac{\partial N_j}{\partial z}+N_i\frac{\partial N_j}{\partial z}q_z\right)dz;$$

$$\left[Q_{ij}\right]=\sum_{e}\int_{z=0}^{z=L}N_iN_j\theta\kappa dz;$$

$$\left[R_{ij}\right]=\sum_{e}\int_{z=0}^{z=L}N_iN_j\theta\kappa\lambda dz; \qquad \textit{and}$$

$$\left\{S_i\right\}=N_iD_z\left(\frac{\partial C}{\partial z}\right)\Bigg|_{z=0}^{z=L}$$

The numerical model was coded using the MATLAB technical language. The governed model is named the UNSAT program, which is then employed to estimate the transportation of salt into the soil pore at the unsaturated zone. The UNSAT program contains the subroutine program, which is infiltration water movement (drought), and infiltration-redistribution water movement (heavy rainfall and flood). In this study the, the mode of infiltration-redistribution water movement was chosen to predict the movement of seawater dealing with the capillary force and percolation. As there is the effect of capillary rise, which can withdrawn the seawater into soil pore via the capillary force. Besides, the UNSAT model is developed to estimate the migration of salt into soil layer at the unsaturated zone.

2.7 Summary

The change of climatic condition can disturb the balance of hydtrological cycle, shifting the massive of water from land to sea. The sensitive areas are the aquifer at the Thailand Gulf and the mangrove forest at Phetchaburi, Thailand. The salt can transport landwards or seawards, due to the magnitude of freshwater from rainfall. If there is drought, the salt intrusion may be occurred. If there is heavy rainfall or flood, the salt extrusion may be faced. Besides, the sea level is another key issue, responding the salt transport. If there is stagnant sea level, the flux of seawater may be constant. In case of sea level rise, the salt transport may be highly influenced by the fluxes of seawater. The set of governing equations are reviewed to construct the mathematical model. The UNSAT program is applied in this study to predict the salt transport under the changing of climatic conditions.

CHAPTER 3 EXPERIMENTAL SETUP

3.1 Overview

The aim of this research is to predict the transportation of salt under various conditions, which are the side effects of climate change. The experiments are designed to simulate the possible pattern of salt migration under three critical conditions, which are drought with stationary sea level, drought with sea level rise and flood with stationary sea level. The experiments are included three major parts, which are the determining the constants for the hydraulic properties model, the estimating of salt migration under various critical condition and model applications. The tests are carried on the laboratory columns, the procedure of experimental setup is described as follows.

3.2 Sand and soil sample preparation

Sand and soil samples are employed to the study to simulate the sandy and silty aquifers, which are at Thailand Gulf and mangrove forest at Phetchaburi, Thailand, respectively. To obtain the nature condition of coastal sandy aquifer, the sand sample is sieved to sort the medium grain sand with particle sizes of 0.20 and 0.50 mm (200-500 μm). The river sand is introduced to this study as it is free from salt, which can eliminate the interrupting in the background concentration of infiltration. The soil sample is collected from agricultural area at Bangkhuntien, which is closed to Thailand Gulf. The soil sample is classified as silt, which can present the silty aquifer at the mangrove forest, in Phetchaburi, Thailand. The soil sample is sieved to eliminate the impurities. The particle size of soil is between 0.20 and 0.50 mm. The characteristics of sand and soil samples are determined by followed the ASTM Standards. The parameter and methods of sand and soil properties determination are shown in Table 3.1.

Table 3.1 Parameter and analytical methods for soil properties testing

Parameter	**Analytical method**	**Reference**
Physical properties		
Particle size distribution	Sieving in combination with hydrometer method	ASTM (1997)
Hydraulic conductivity	Standard test method for permeability	ASTM (1997)
Bulk density	Sand density method using Archimedes Principle	ASTM (1997)
	Soil particle density	ASTM (1997)
Specific gravity	Oven drying method	Gardner (1965)
Soil water content		
Chemical properties		
Electrical Conductivity, EC	Conductivity meter method	Jackson (1967)

The physical appearances of sand and soil samples are illustrated in Figure 3.1.

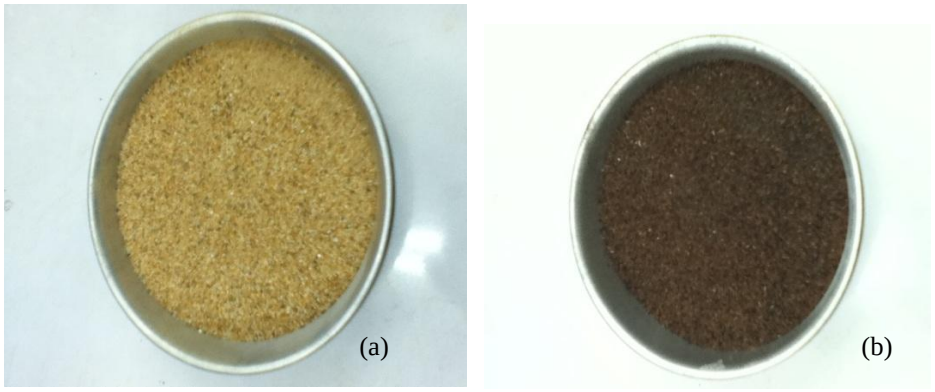

Figure 3.1 Physical appearances of porous materials (a) sand and (b) soil

3.3 Freshwater and saltwater preparation

By definition, freshwater and seawater can be accounted by the level of sodium chloride (NaCl). The freshwater contains no sodium chloride, the brackish water contains sodium chloride less than 35 permille (35 g/L), and seawater contains sodium chloride more than 35 permille. The freshwater utilised in this study is the deionised water, as it is free from sodium chloride. The seawater is synthesised by diluting the 35 g of sodium chloride in a litre of deionised water. The food grade dye is added into the synthesis seawater, to make the obvious colour. For the sake of naked eye observation, the

interface between freshwater and saltwater may be observed by the colour of saltwater. In every batch of deionised water and synthesis seawater the level of NaCl is measured by the electrical conductivity, to confirm the level of salinity of infiltration and seawater.

3.4 Sand and soil column test

The laboratory scale soil columns are made of the acrylic tubes, with the diameter of 6.5 cm and the depth of 35 cm. The sand and soil samples are randomly packed into the columns with controlling the bulk densities of 1.56 and 1.11 g/cm^3, respectively. The tests are included two parts, which is the determination of constants for the hydraulic properties model and estimating the salt transport under various environmental conditions.

3.4.1 Determination of hydraulic properties model

The experimental setup is described in Figure 3.2.

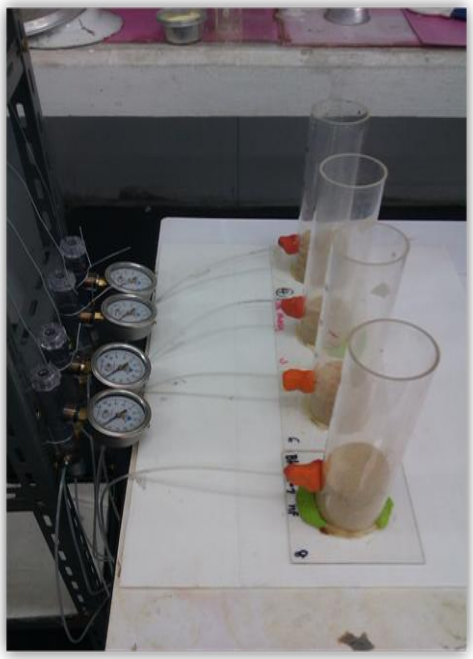

Figure 3.2 The soil hydraulic properties test

The sand and soil columns are prepared carefully, the sand and soil sampled are packed with a 6 cm thick. This thin layer of sand and soil samples may be assumed to be

homogenous layer of porous media, which is presented in unsaturated zone. The single jet-fill tensiometer, model 2100F is placed at the centre of column at the elevation of 3 cm above the column base. The test is operated under the drying cycle and the freshwater is filled gradually into the column at the surface. The sand and soil specimen are taken in every hour interval to analyse the volumetric moisture content, and the pressure head is recorded in every hour interval. The data of volumetric moisture content and pressure head are plotted and the relation between these parameters is determined by van Genutchen model.

3.4.2 Evaluating seawater transportation

The columns are prepared with the same manner as the previous test. The sand and soil samples are filled into the columns with controlling bulk densities at 1.56 and 1.11 g/cm^3, respectively. The packing height of column is 20 cm. The series of jet fill tensiometers, model 2100F are placed at the centre of column, at the elevations of 3, 6, 9, 12, 15 and 18 cm above the column base (datum).

According to the changing of climatic condition, the hydrological cycle may be shifted and the sea level may be arisen. The assigned conditions are drought with stationary sea level, drought with sea level rise and flood with stationary sea level are employed to be the boundaries of this study. The procedures for column tests are explained as follows.

1) Drought with stagnant sea level

At the equator and tropical zone, the rainfall intensity may be declined 10-25% from the present. The reduction of rainfall intensity is caused by climate change phenomena (Nigel, 1999). To simulate the salt migration in unsaturated zone, under drought condition, the sand and soil samples are packed into the column with a packing depth of 20 cm. The packed sand and soil columns have the bulk densities at 1.56 and 1.32 g/cm^3, respectively. The columns are placed at the seawater tank, the synthesis sweater is filled to the level of column base (datum). This can be assumed as at elevation of 0 cm (z=0 cm). As there is no rainfall during the dry season, there is no freshwater adding at the column surface. In every hour interval, the samples are removed from the column and determined for EC(1:5). The samples are separated for every 4 cm interval. The

tests are conducted until achieving the steady state of inflow-outflow. The experimental set up is shown in Figure 3.3.

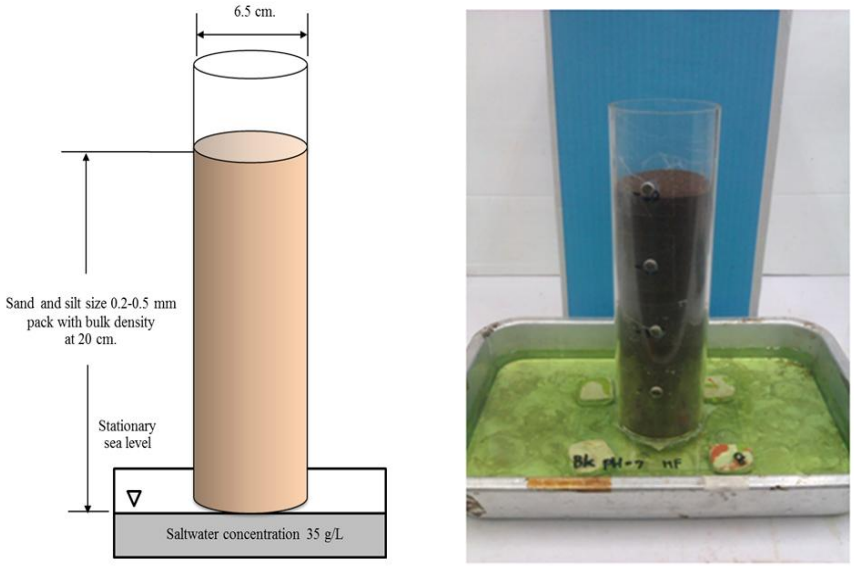

Figure 3.3 Column test under drought with stationary sea level

2) Drought with sea level rise

According to the IPCC (2007), the prediction of se level in year 2100 may be increased 0.11-0.88 m from the present. To simulate the effect of sea level rise in the salt transport, the columns are prepared as previous tests. The columns are placed at the synthesis seawater tank, and the level of synthesis seawater is maintained at 2 cm above the datum (z=2 cm). The sea level is increased at 10% of total depth of unsaturated zone. The tests are conducted until the system reaches the equilibrium of inflow-outflow. The sand and soil samples are removed for every an hour interval, the specimen are separated for every 4 cm deep, they are examined for the EC(1:5). The experimental setup is illustrated in Figure 3.4.

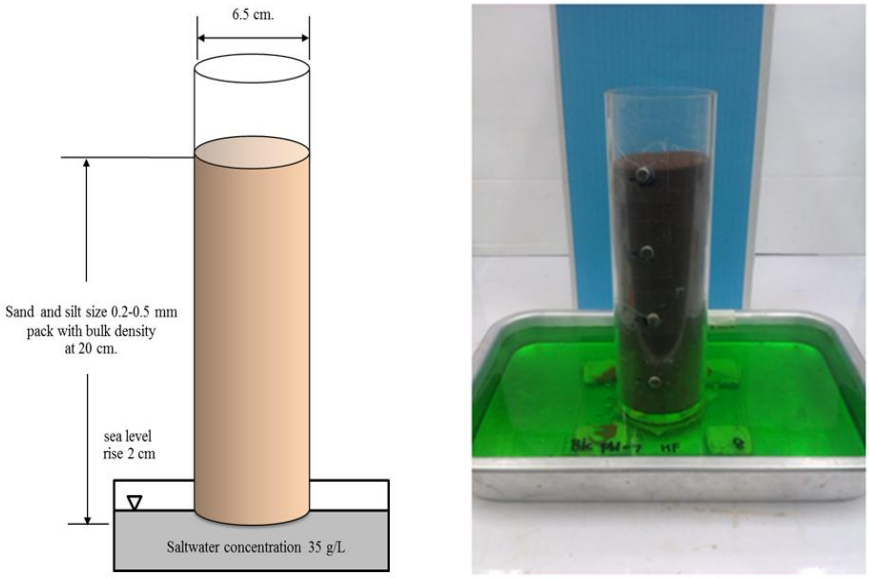

Figure 3.4 Column test under drought with sea level rise

3) Flood with stagnant sea level

In case of heavy rainfall, the rainfall intensity may increase 13-18% from the present (Nigel, 1999). The unsaturated zone may suffer from flood. To simulate this critical scenario, the sand and soil columns are prepared as same as the previous test. The column was placed into the synthesis seawater tank, maintaining the seawater level at the datum (z=0). The freshwater is sprayed on the column surface at the rate of 80 cm^3/d, equalled a daily rainfall intensity at 2.41 mmH_2O. By observation, there is ponding of freshwater at the top of column surface and the depth of ponding water is 2.41 cm. This can be assumed that the unsaturated zone may possibly suffer by heavy rainfall and the flood may be occurred, when the climatic condition is shifted. The tests are employed until achieveing the steady state of inflow and outflow. The samples are removed in every hour interval, and then it is separated into the 4 cm thick layer of sample. The specimen are test for EC(1:5) to determine the NaCl distribution curve. The experimental setup is illustrated in Figure 3.5.

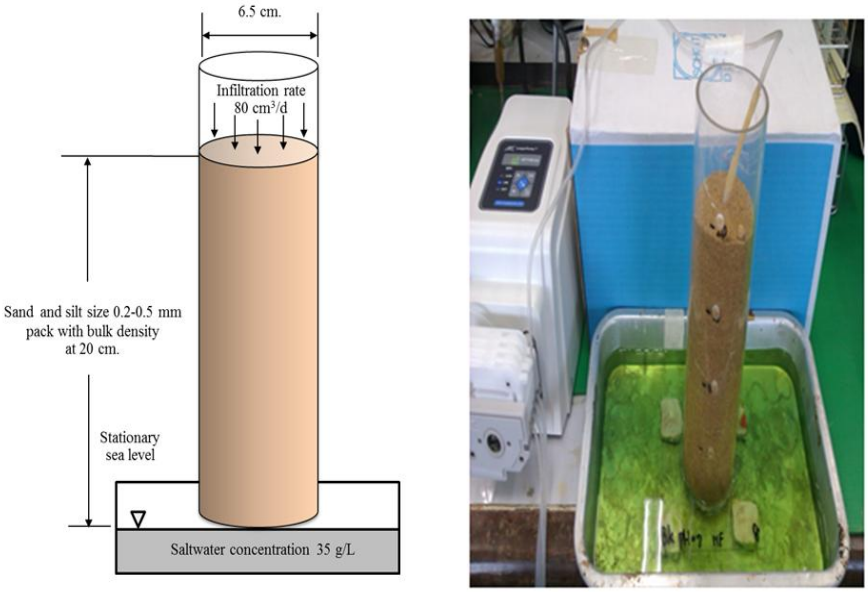

Figure 3.5 Column test under flood with stationary sea level

A conceptual model of saltwater intrusion under various environmental conditions is present in Figure 3.6. In the natural, at the coastal aquifer has presented the interface zone which separated freshwater and saltwater. The interface zone is controlled by fluxes of freshwater and seawater. Under the critical scenarios, the drought may reduce the flux of freshwater resulting in the salt intrusion. On the other hand, the heavy rainfall or flood can increase the flux of freshwater and this can bring the salt extrusion. Besides, the sea level also controls the flux of seawater. The stationary sea level could bring the hydrodynamic force, which can push the freshwater floating and flowing horizontally. When the sea level in increased, the flux of inflow at the side of seawater is increased, bringing the salt intrusion. However, the sandy and silty aquifers may show the different patterns of salt migration and the depth of interface between freshwater and seawater may be different. Since the silty aquifer may present the low permeability, which can retard the creeping of seawater towards the land. However, the sand aquifer may present the high permeability, the freshwater may percolate rapidly. This system may present the low salinity in the unsaturated zone. Since, the porewater in the unsaturated zone can be accounted as the available water for plants. If the freshwater inside the soil pore is contaminated with seawater, it can destroy the costal ecological system and eventually the marine ecological systems.

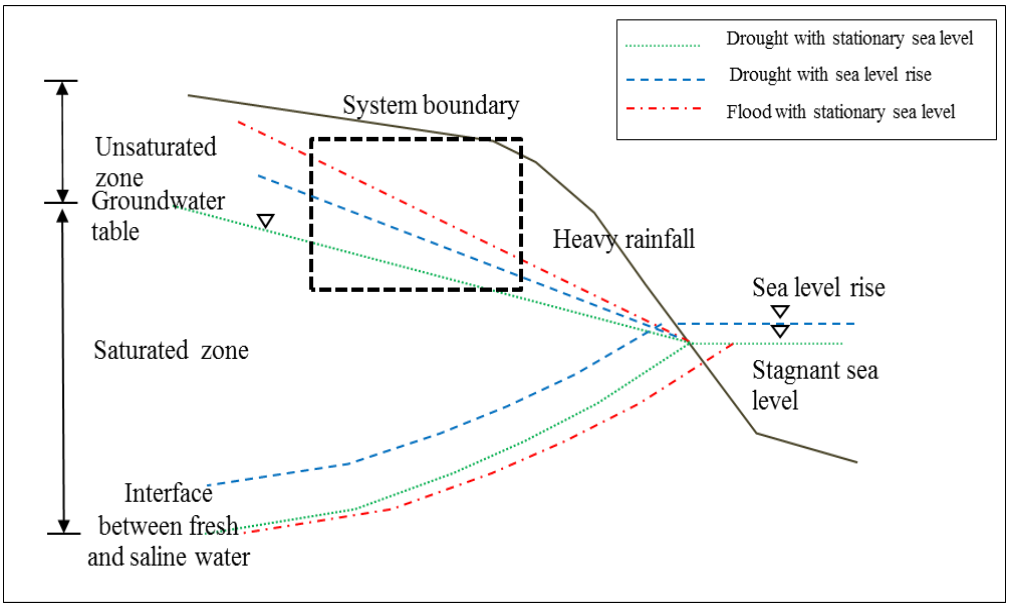

Figure 3.6 Conceptual model of saltwater intrusion

3.5 Model Application

The boundaries conditions and the constants for hydraulic properties model governed from the previous tests are input to the UNSAT program. The considered areas in this study are the coastal aquifer at Thailand Gulf and mangrove forest at Phetchaburi, Thailand. As presented in the reports, the aquifer thickness at Thailand Gulf is 20-80 m and the averaged thickness is 45 m. The aquifer is counted as unconfined aquifer with single layer of sand porous material. The unsaturated zone at this area is 5-12 m deep. Based on the prediction results, the critical scenarios of unbalance hydrological cycle under climatic change can be either drought or flood. The climatic model predicted that the rainfall intensity may either reach to 80 mm/day or be low rainfall intensity of 0 mm/d within 2050 and the sea level rise will be 0.11 – 0.88 m in 2100 in the tropical zone. The domain of aquifer is scaled up and the same boundaries conditions are employed to predict the salt movement along Thailand Gulf in year 2100. The concept for model applications is drawn in Figure 3.7.

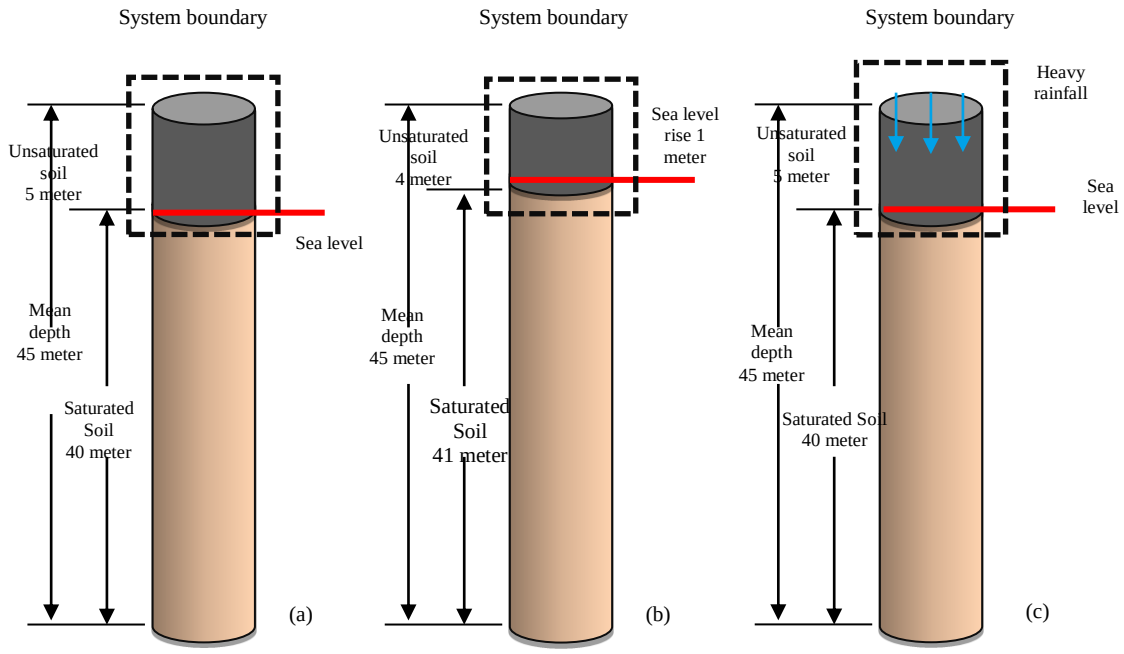

Figure 3.7 Model applications in salt migration at Gulf of Thailand (a) drought with stationary sea level (b) drought with sea level rise and (c) flood with stationary sea level

Another concern is the salt migration in unsaturated zone at the mangrove forest, in Phetchaburi, Thailand. Based on the geographical data, the aquifer thickness at this area is only 50 m, and the averaged thickness is 10 m. The unsaturated zone is 0.5-1.5 m deep. The aquifer is classified as unconfined aquifer, the silt is predominant material. This silty aquifer may suffer from the changing of climatic conditions as same as the coastal aquifer at Thailand Gulf. Three environmental conditions, which are drought (0 mmH_2O/d rainfall intensity) with stationary sea level, flood (80 mmH_2O/d rainfall intensity) with sea level rise (0.88 m above the datum) and flood with stationary sea level are bound. The constants for hydraulic properties model and the boundary conditions are fitted as same as the previous tests. The conceptual model for prediction of salt migration in unsaturated zone is described in Figure 3.8.

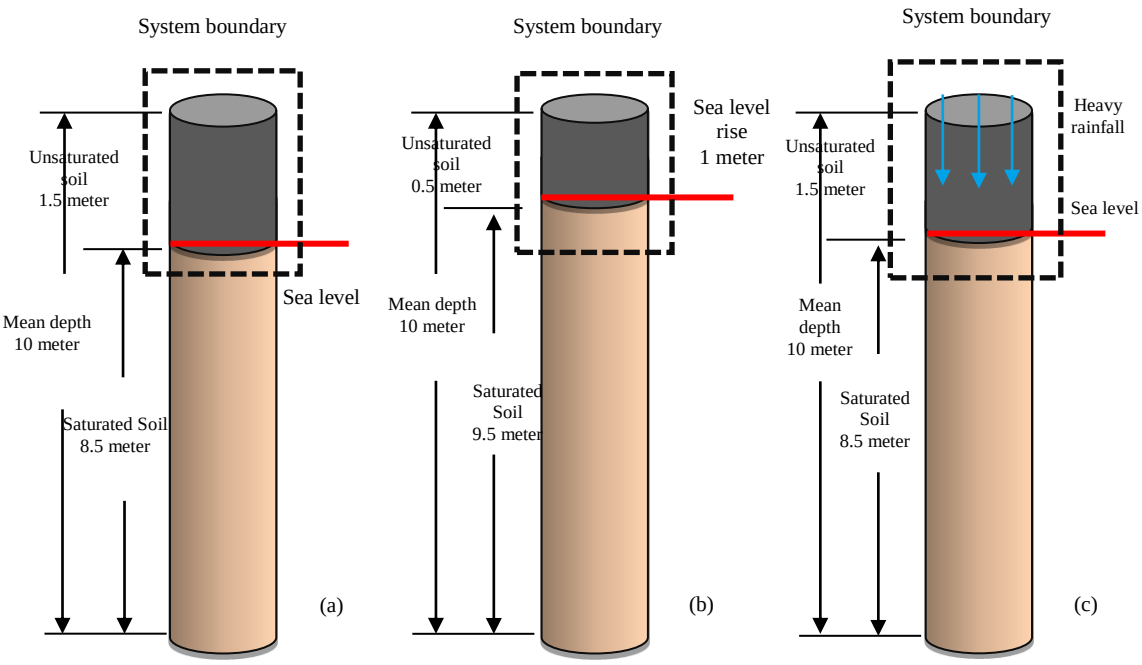

Figure 3.8 Model applications in salt migration at mangrove forest (a) drought with stationary sea level (b) drought with sea level rise and (c) flood with stationary sea level

CHAPTER 4 RESULT AND DISCUSSION

4.1 Sand and soil sample characteristics

The sand and soil samples used in this research were from river sand and agriculture soil (organic soil). Both samples have an averaged particle diameter of 0.2-0.5 mm. The physical and chemical properties are analysed in concordance with the ASTM standards as shown in Table 4.1. The raw data is presented in Appendix A.

Table 4.1 Physical and chemical properties of sand and soil sample

Parameter	Type of material	
	Sand	Soil
Physical properties		
Bulk density (g/cm^3)	1.56	1.11
Specific gravity	2.56	1.22
Water content (%)	1.00	3.89
Hydraulic conductivity (cm/hour)	0.25	0.18
Soil texture (%)		
Sand	96.89	10.40
Slit	3.11	86.9
Clay	0.00	0.00
Soil classification	Sand	Silt
Chemical properties		
Electrical Conductivity, EC(1:5) (µs/cm)	40.26	3667
Saturated EC, EC_e (µS/cm)	503	22002
NaCl content (equivalent to gNaCl/L)	0.33	14.46
Salinity (‰)	0.00	1.50
pH	6.73	6.40

The river sand sample and agricultural soil sample are classified as sand and silt, respectively. The bulk density of river sand sample is higher than silt sample. This indicates that the silt sample may looser than sand, and it could be consolidated rapidly whenever the hydraulic load is applied. In case, the spraying freshwater at the column surface is accumulated as ponding water, the silt particle may be packed and becomes denser layer of silt aquifer. According to the specific gravity of sand and silt particles,

the higher specific gravity is observed in sand sample. This suggests that the sand particles are rigid, but the silt particles are soft. Therefore, the sand particles do sorb the water with a less amount than the silt particles. The water content of sand particles is much lower than the silt particles. In accordance with sorptive capacity of silt particles, the low amount of water can penetrate the pore. Indeed, the hydraulic permeability of silt particles should be much lower than sand particles. However, the silt particles had a slightly lower permeability than the sand particle, it might be possible that the layer of silt was too loose, the size of effective pore might be large. Beside, the layer of silt particles could easily absorb and desorb water very quickly, its behavior looked similar to sponge. Almost of pores of silt particles are held the water in very long period. Besides, silt particles contain the cations, which can present the high value of EC(1:5). Some cations are classified as salt, the soil salinity is high. It is equivalent with a concentration of 1.50 gNaCl/L, which is a slightly sodic soil.

4.2 Freshwater and seawater characteristics

The deionised water is applied as freshwater and the synthesis seawater is prepared by adding 35 gNaCl into 1 L of deionised water. The properties of freshwater and synthesis seawater are presented in Table 4.2.

Table 4.2 Freshwater and saltwater characteristics

Parameter	Freshwater	Saltwater
Conductivity (mS/cm)	0	56.58
NaCl content (g/L)	0	37.2
Temperature (^{o}C)	25	25
Density (kg/L)	0.997	1.025

The freshwater sample is free from NaCl. The seawater is synthesized from commercial salt, which is food grade quality. The salt contains 99.999% NaCl, hence the concentration of NaCl of the synthesis seawater is closed to the real seawater. Besides, the densities of freshwater and seawater may varied by the temperature. Hence, the detected data is undertaken at standard temperature of 25 ^{o}C. The density of seawater is slightly higher than the freshwater. Salt with a higher density may sit down at the saltwater tank without stirring. This could simulate the real condition that can present the density dependent flow condition without effect of wave and erosion.

As the concentration of NaCl is correlated well with the electrical conductivity (EC) well, the function of concentration of NaCl and EC is defined as shown in Figure 4.1. Hence, the concentration of NaCl can be obtained by converting the measured value of EC via this standard curve. This could not disturb the flow of sample and it can be measured at the real time.

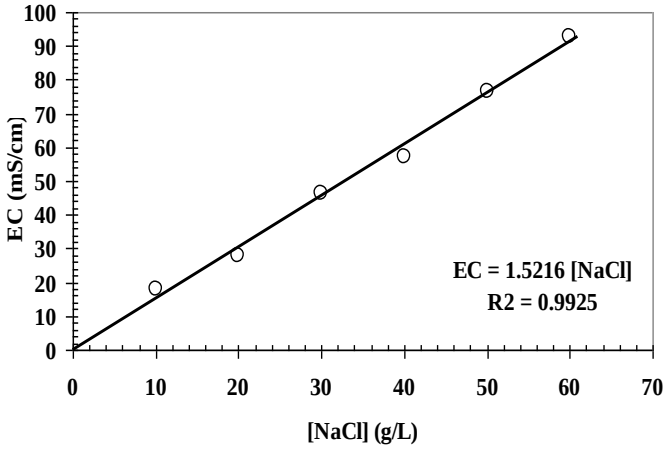

Figure 4.1 Standard curve of concentration of NaCl versus electrical conductivity

The soil columns test are conducted to determine the constants for hydraulic properties model and to observe the salt migration at various environmental conditions. The tests are employed to simulate the salt distribution inside the soil pore under three different conditions, drought with stationary sea level, drought with sea level rise and flood with stationary sea level.

4.3 Hydraulic properties curve

The hydraulic properties curve was prepared to convert the pressure head to volumetric water content. The constants for hydraulic properties curve was obtained by van Genuchten's model. The hydraulic properties curve is given in Figure 4.2. The constants for hydraulic properties are summarised in Table 4.3. The obtained constants for hydraulic properties were closed to the ones referenced by Carsel and Parrish.

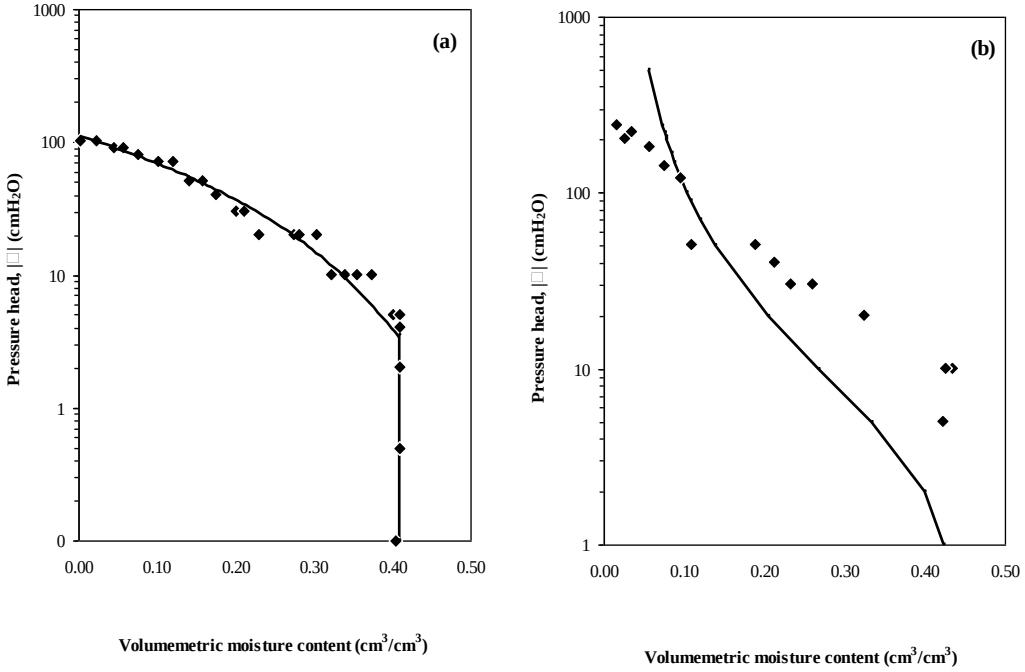

Figure 4.2 Water retention curve (a) sand sample and (b) soil sample

Table 4.3 Constants for hydraulic properties

Parameter	Sand sample		Soil sample	
	Reference value	**Calculation**	**Reference value**	**Calculation**
θ_s	0.430	0.403	0.460	0.441
θ_r	0.045	0.043	0.034	0.014
a	0.145	0.045	0.106	0.132
p	2.686	2.080	1.370	1.480
m	0.626	0.521	0.403	0.324
Kz (cm/hour)	-	0.250	-	0.180

By observation, the sharp front located between saturated and residual volumetric water contents was observed in the silt sample. As expected, the layer of silt could behave as sponge. The infiltration water could rapidly absorb at initial stage. As soon as the pore was full with water, the cumulative water could move downwards under gravitational force. Hence, the hydraulic properties curve for silt sample had shown in the shaped of inverted s-curve. On the other hand, the hydraulic properties curve of sand did not present the complete inverted s-curve. The sharp front was not obtained as the water inside the sand was balanced by the surface tension and gravitational force. The uniform flow was observed in the layer of sand due to the uniformity of sand particles.

4.4 Sand column test

The observations from laboratory scale soil column tests are included the seawater distribution along the unsaturated soil layer. There are three environmental conditions, which are drought with stationary sea level, drought with sea level rise and heavy rainfall with stationary sea level. The observations are compared with the simulations cases by cases, as described as follows.

4.4.1 Drought with stationary sea level

The test for seawater redistribution under capillary rise was firstly conducted under the stationary sea level condition. The hydraulic pressure head was linearly distributed along the column's elevation. The soil moisture content distribution was obtained by converting the hydraulic pressure head to volumetric moisture content via the hydraulic properties model of van Genuchten. This observation was applied as the boundary condition of the test of salt intrusion model. The inputs for model simulation are given in Table 4.4.

Table 4.4 Inputs for seawater movement under drought with stationary sea level

Parameter	Values
Domain	20 cm thick sand layer
Total considered period	1 hour
Number of time step	120
Hydraulic properties model	van Genuchten (constants are in Table 4.3)
Boundaries condition	Hydraulic pressure head at the surface and the base of column were -11.5 and 0 cmH_2O, respectively.

The simulation results for hydraulic pressure head and volumetric water content distributions under drought with stationary sea level are presented in Figure 4.3. The simulation well agreed with the observation. Only 2 cm of sand layer at the base of column was fully saturated. The sand column surface was slightly wet due to the capillary rise. The intermediate zone between sea level and unsaturated zone was balanced under the redistribution of sea water and the gravitational flow of water, the length of this zone was named as capillary height. The capillary height of this sand column was 12 cm above the datum. This referred that the capillary force could abstract the water from the tank to the height of 12 cm.

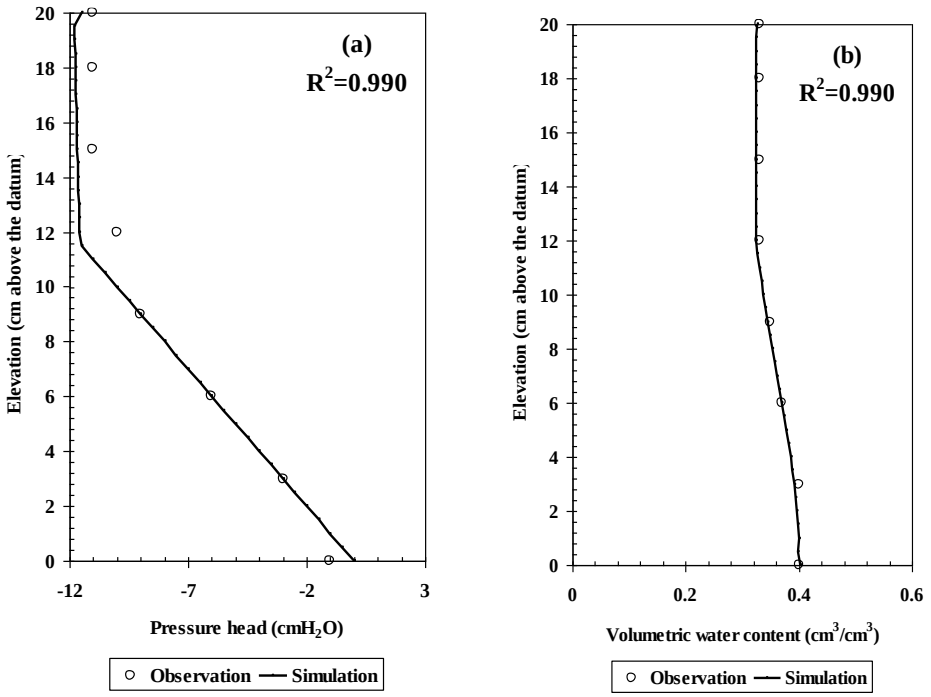

Figure 4.3 Distributions of (a) pressure head and (b) volumetric water content at unsaturated sand layer under drought with stationary sea level

The distribution of NaCl in the sand column is simulated the input is described in Table 4.5.

Table 4.5 Inputs for NaCl distribution under drought with stationary sea level

Parameter	Values
Domain	20 cm thick sand layer
Total considered period	1 hour
Number of time step	120
Boundaries condition	The concentration of NaCl at the column base is 35 g/L. The initial concentration of NaCl is 0.33 g/L.
Molecular diffusion	0.04788 cm^2/h

The NaCl could move upwards to the column surface, the interface between fresh and salt water was at 1 cm above the datum. It could suggest that the capillary force may withdraw water very quickly, but the migration of NaCl through the soil pore may be retarded by the dispersion mechanism. The observation and simulation results are presented in Figure 4.4. The simulation could be well corresponded to the observation data. However, the loss of NaCl along the sand pore may be occurred due to the dispersion process. The explanation

of NaCl may be observed in both vertical and horizontal directions, as the colour of seawater is vanished along the sand column.

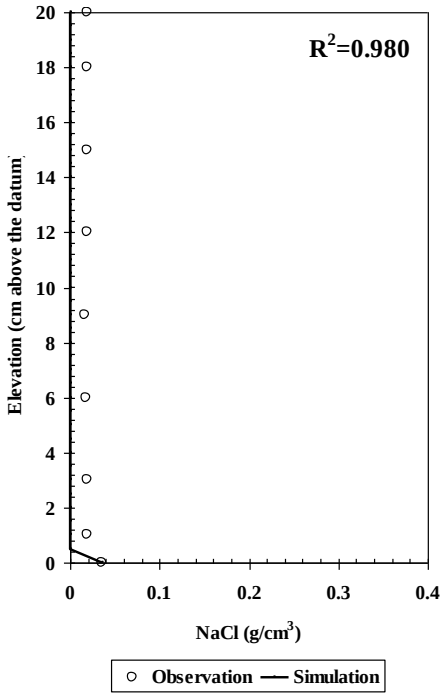

Figure 4.4 Distribution of NaCl at unsaturated sand layer under drought with stationary sea level

4.4.2 Drought with sea level rise

Table 4.6 presents the input for seawater movement under drought with sea level rise. The simulations for drought with sea level rise are presented in Figure 4.5.

Table 4.6 Inputs for seawater movement under drought with sea level rise

Parameter	Values
Domain	20 cm thick sand layer
Total considered period	1 hour
Number of time step	120
Hydraulic properties model	van Genuchten (constants are in Table 4.3)
Boundaries condition	Hydraulic pressure head at the surface and base of column were -10.5 and 0 cmH_2O, respectively. The capillarity pressure head distribution was applied as the initial condition.

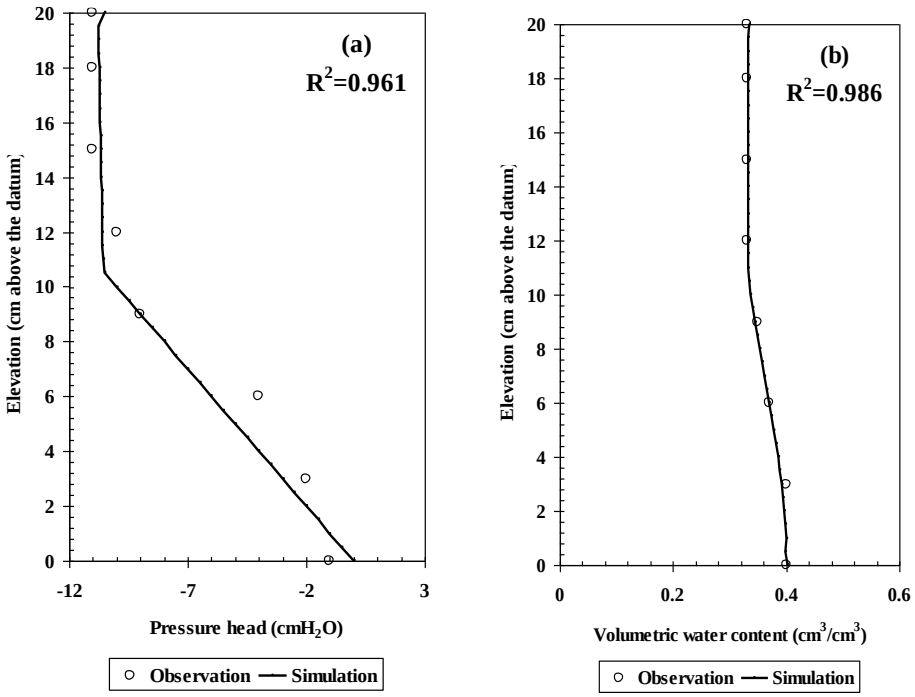

Figure 4.5 Distributions of (a) pressure head and (b) volumetric water content at unsaturated sand layer under drought with sea level rise

The moisture distribution was silimar to the previous case with stationary sea level. However, the moisture content at the column surface was increased slightly. The redistribution was increased due to the increase of piezometric hydraulic head. The height of capillary rise was constant at 10 cm above the datum. This confirmed that moisture content of sand was still controlled by the capillary force. Besides., the distribution of NaCl along the sand column is considered, the input parametrs are presented in Table 4.7. The results are provided in Figure 4.6.

Table 4.7 Inputs for NaCl distribution under drought with sea level rise

Parameter	Values
Domain	20 cm thick sand layer
Total considered period	1 hour
Number of time step	120
Boundaries condition	The concentration of NaCl at the column base is 35 g/L. The initial concentration of NaCl is 0.33 g/L.
Molecular diffusion	0.04788 cm^2/h

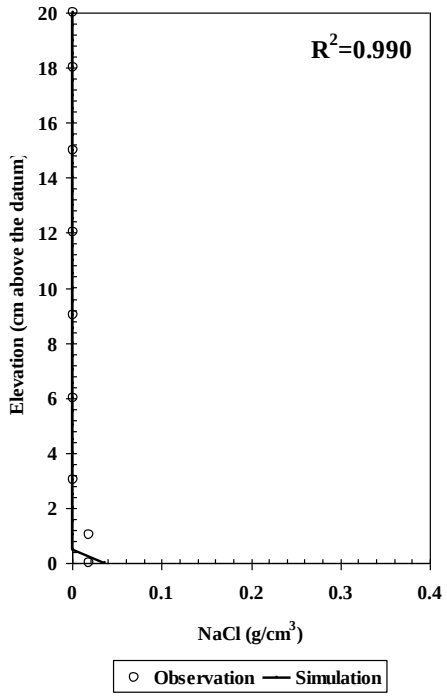

Figure 4.6 Distribution of NaCl at unsaturated sand layer under drought with sea level rise

The concentration of NaCl profile in the soilpore was remained constant at the same level as the previous condition, which was 1 cm above the datum. This assumed that the micropores of sand could behave as the microfilter, which could separate the NaCl and water for some short distance via the dispersion mechanism. It could believe that even the sea level was arisen, the interface between seawater and freshwater did not significantly move upwards. This could imply that the capillary force may influence the movement of seawater along the soil pore.

4.4.3 Flood with stationary sea level

The simulations of water content distribution and NaCl concentration profile under flood were undertaken. The simulation of inflows of freshwater and seawater through the sand column was observed by inputting the parameters as displayed in Table 4.8.

Table 4.8 Inputs for inflows of freshwater and seawater under flood with stationary sea level

Parameter	Values
Domain	20 cm thick sand layer
Total considered period	1 hour
Number of time step	120
Hydraulic properties model	van Genuchten (constants are in Table 4.3)
Boundaries condition	Hydraulic pressure head at the surface and the base of column were 0.00 and 0.00 cmH_2O, respectively. The capillarity pressure head distribution was applied as the initial condition.

The distributions of pressure head and volumetric water content are presented in Figure 4.7. The water content was increased at the column surface due to infiltration. The inflow moved downwards due to gravity force in the meantime the seawater moved upwards due to capillary force. The water content of sand was increased sightly at every elevation.

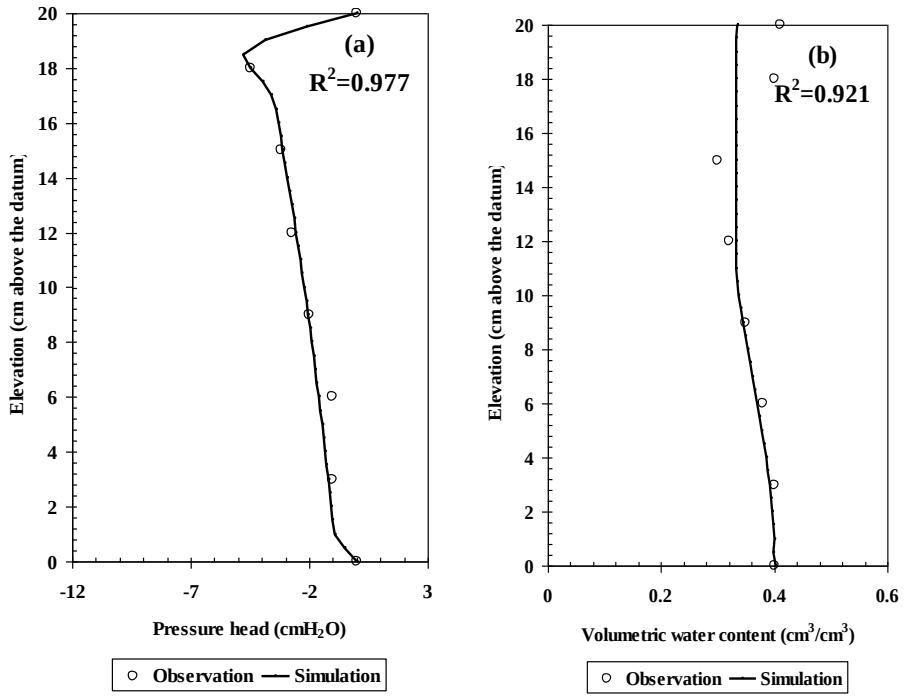

Figure 4.7 Distributions of (a) pressure head and (b) volumetric water content at unsaturated sand layer under flood with stationary sea level

The input for NaCl distribution under flood and stationary sea level is provided in Table 4.9 and the profiles of NaCl concentration is illustrated in Figure 4.8.

Table 4.9 Inputs for NaCl distribution under flood with stationary sea level

Parameter	Values
Domain	20 cm thick sand layer
Total considered period	1 hour
Number of time step	120
Boundaries condition	The concentration of NaCl at the column base is 35 g/L. The initial concentration of NaCl is 0.33 g/L. The concentration of NaCl at the column surface is kept at 0.0 g/L
Molecular diffusion	0.04788 cm^2/h

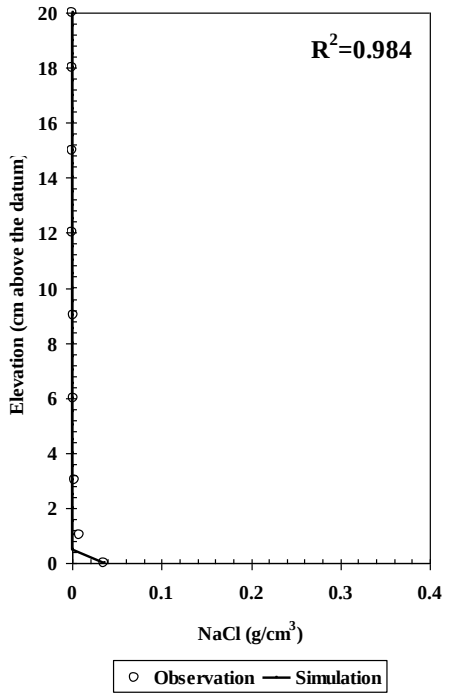

Figure 4.8 Distribution of NaCl at unsaturated sand layer under flood with stationary sea level

The concentration of NaCl profile in the soil pore was reduced as a result of diluting. The concentration of NaCl profile indicated thant less than 0.4 cm of sand layer above the datum contaminated with NaCl. So, the heavy rainfall can increase the inflow, the freshwater can flush the saltwater. The interface between seawater and freshwater significantly moves

downwards. This could imply that the magnitude of inflow could overcome the capillary force, resulting in salt extrusion.

The UNSAT program could respond to the observations of pressure head distribution, volumetric water content distribution as well as the the NaCl concentration profile under the critical environmental condition. The program had presented the constants for each case, such as Darcy's velocity, averaged volumetric moisture content and NaCl dispersion coeffient, which were useful to magnitude the migration of seawater at unsaturated sand layer. These constants are provided in Table 4.10.

Table 4.10 Constants for seawater movement in unsaturated sand layer

Parameter	**Unsaturated sand layer with**		
	Drought and stationary sea level	**Drought and sea level rise**	**Flood and stationary sea level**
Darcy's velocity (cm/h)	-0.0017	-0.0026	-0.0831
Averaged volumetric moisture content (cm^3/cm^3)	0.3592	0.3625	0.4028
NaCl dispersion coefficient (cm^2/h)	0.0324	0.0390	0.5450

The negative Darcy's velocity was obtained in every test. The negative Darcy's velocity had presented the downward flow of system, due to the suction head. In case of drought with stationary sea level, the velocity of seawater moved upwards was the slowest. Almost of water move upwards was occurred by the capillary rise. When the sea level rise, the elevation head could drive the seawater went through the unsaturated sand layer more quickly than the case with stationary sea level. The downwards flow of seawater may be a result of gravitation flow. When the seawater was more accumulated in the sand pore, the surface tension of sand pore may overcome. The seawater tended to outflow under gravitational force. On the other hand, the flood with stationary sea level, the highest Darcy's velocity was shown. This referred that the flux of freshwater could penetrate the sand pore and washed out the accumulated seawater inside the sand pore. Besides, the

averaged volumetric moisture contents were confirmed that the case of flood with stationary sea level, the sand pore was almost filled with freshwater. The volumetric moisture content had shown the highest value. The averaged volumetric moisture content of sand under drought with stationary sea level was slightly lower that the one under drought with sea level rise. This suggested that the seawater could bring and be accumulated inside the sand pore, when the elevation head of inflow of seawater was increased. The sand pore was filled with seawater and this case could harm the availability of freshwater in the sandy aquifer. Moreover, the NaCl dispersion coefficient could describe the extension of NaCl flume. The unsaturated sand layer could be highly suffered, when it was under drought with stationary sea level. As the accumulated NaCl inside the soil pore did not extent to the other area. When the NaCl content was high enough to be deposited, the salt rock may be observed. Similarly, the NaCl was slightly dispersed when there was drought with sea level rise. The NaCl could slightly migrate due to the molecular diffusion. However, The sand pore may be occupied with concentrated NaCl, and eventually forming the salt rock. Unlikely, the NaCl was removed by inflow of freshwater, whenever the rainfall intensity was high or flooding. The NaCl could highly disperse due to both mechanical and molecular diffusion processes. Hence, the sand pore may be free with seawater.

According to the observation and simulation, the drought with sea level rise was the most critical situation. Since, the NaCl could contaminate the freshwater inside the sand pore and the flume of NaCl was less expanded. The accumulated NaCl could be formed as salt rock and the sandy aquifer became salty water permanently. This situation could pose the most serious impact to ecological cycle. If the coastal aquifer was under drought condition, the artificial recharge of freshwater may be recommended to relieve the impact of salt intrusion.

4.5 Model applications for sandy aquifer

The evaluations of salt migration at the coastal aquifer along the Gulf of Thailand are predicted under various environmental conditions. There were drought with stationary, drought with sea level rise and heavy rainfall with stationary sea level. The predictive results are shown the possible seawater migration within year 2100. The results were explained as follows.

4.5.1 Drought with stationary sea level

Increasing of global temperature could stimulate the evaporation rate of water in ocean and surface water and the melting of glaciers. The unbalance hydrological cycle could bring either flood or drought. The prediction indicates that 10-25% rainfall intensity will be declined along the areas located at the equator and tropical zone (Arnell, 1999). The input parameters are same as the tests of sand column under drought with stationary sea level as presented in Table 4.4. Only the considered domain was extended to the elevation of 500 cm above the water table. The simulation results for distributions of pressure head and volumetric water content are illustrated in Figure 4.9.

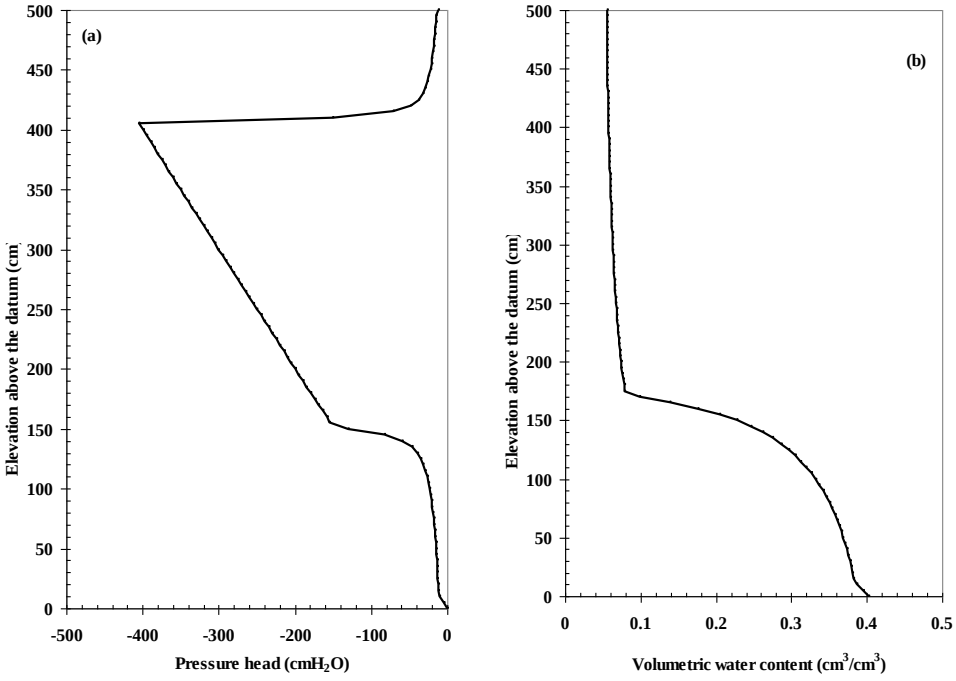

Figure 4.9 Simulation of seawater movement at coastal sandy aquifer (a) pressure head distribution and (b) volumetric water content distribution under drought with stationary sea level

The simulation had shown that the capillary rise can abstract the saltwater to the elevations of 150 cm above the datum. A sharp dried sand pore may be observed at the elevations between 150 and 400 cm above the datum. Above the elevation of 400 cm above the datum, the accumulated freshwater was stayed. This could indicate that the capillary force can abstract the seawater. At the elevation of 150 cm, the seawater could fill almost the sand pore. The aquifer at the elevation 0-150 cm was closed to the water table and

saturation zone. This might be accounted as the smearing zone, which NaCl could be moved either upwards or downwards, depending on the sea level. The simulation for NaCl concentration profile was employed, the input parameters were same as the previous case of drought with stationary sea level as summarised in Table 4.5. The simulation results for NaCl concentration profile are shown in Figure 4.10.

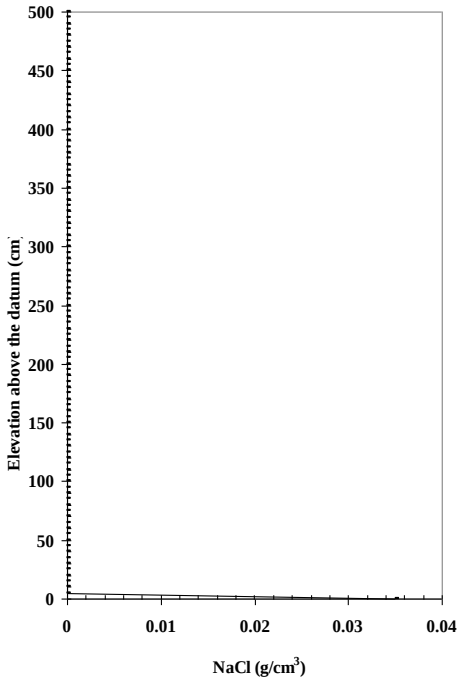

Figure 4.10 Simulation of NaCl concentration profile at coastal sandy aquifer under drought with stationary sea level

The simulations suggested that the NaCl could contaminate the sand porewater at only 10 cm above the datum. Since, the density of seawater is high, the capillary force may be able to abstract the freshwater upwards, but it may not be enough to carried seawater. Hence, the NaCl was naturally deposited at the intermediated zone, locating between unsaturated zone and capillary zone.

4.5.2 Drought with sea level rise

When the temperature is increased, the glaciers will be then melted and the quantity of water in the sea will be expanded. This could increase the volume of seawater and the sea level may be arisen. In the 21st century sea level had been increased for 0.1-0.9 m when the world temperature was increased for 2-5.4 ^{o}C (Arnell, 1999) and the global mean sea level (GMSL) was increased for 3.3 mm per year from 1992 to 2010 (Nicholls

and Cazenave, 2010). By prediction, the global mean sea level may level up more than 110-880 mm within year 2100. The input utilised in this case study was same as the laboratory scale column test. The domain was increased to cape with the 500 cm thick sandy aquifer.

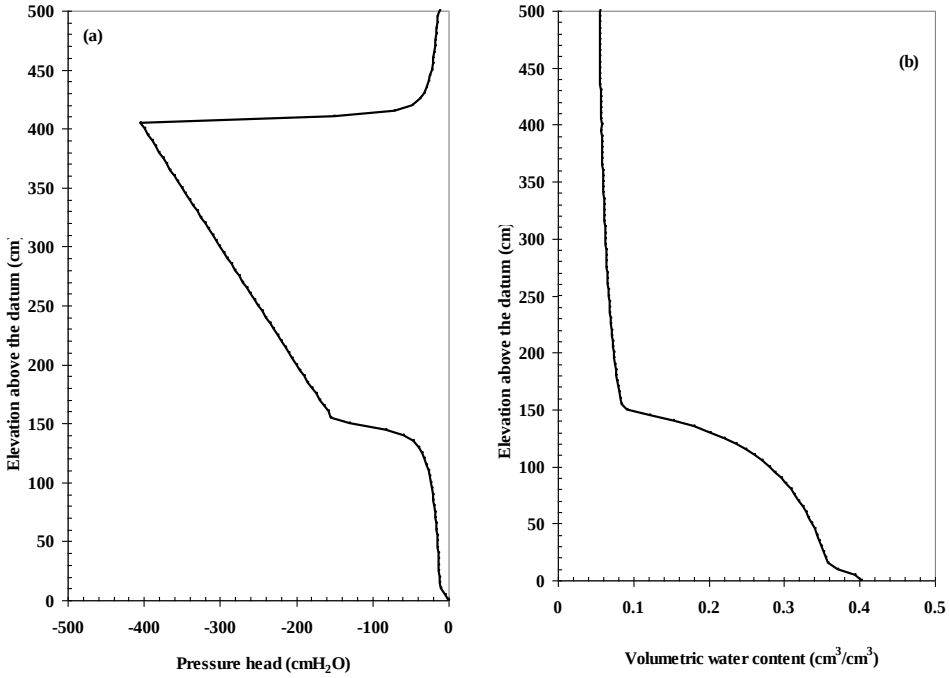

Figure 4.11 Simulation of seawater movement at coastal sandy aquifer (a) pressure head distribution and (b) volumetric water content distribution under drought with sea level rise

According to the pressure head distribution, the seawater could move upwards to the elevation of 150 cm above the datum due to capillary rise and increase of elevation head. The elevations between 150 and 400 cm, the sand pore contained less amount of water. It could behave as the buffer zone between brackish water and freshwater. The freshwater was occupied the sand pore at the elevations 400-500 cm above the datum. However, the moisture content distribution had confirmed that the smearing zone may be at the elevations 0-150 cm above the datum. The movement of salt was represented by the distribution of NaCl. The inputs for NaCl distribution was same as the one, displayed in Table 4.6. The NaCl concentration profile is presented in Figure 4.12.

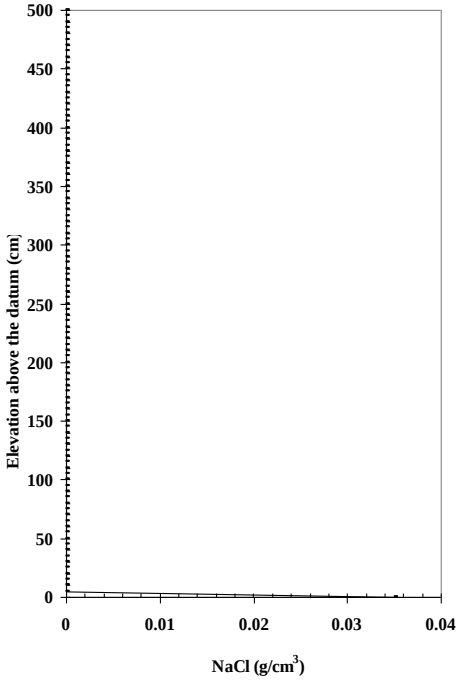

Figure 4.12 Simulation of NaCl concentration profile at coastal sandy aquifer under drought with sea level rise

The profile of NaCl concentration was same as the previous case of drought with stationary sea level. The estimation had indicated that the height of capillary in sandy aquifer along the coastal area seemed to be at the elevations of 1.50 and 1.75 m for cases of stationary and sea level rise, respectively. Besides, the redistribution could bring water through soil matrix, the seepage water tended to move downwards. The arid zone for the case of sea level rise was narrower the natural case of stationary sea level. This could indicate that the capillary force could control the redistribution of salt water through sandy aquifer. The salt could penetrate to the sandy aquifer, the interface between salt and fresh water was observed at the elevation of 0.10 m for both conditions. However, the soil pore water partially contains salt, which becomes the brackish water. This confirmed that the salt intrusion could be controlled by the molecular dispersion and the advection of capillary rise.

Figure 4.13 presents the possible situation of seawater movement, when the area was drought. The sea level may slightly influence the upwards movement of NaCl.

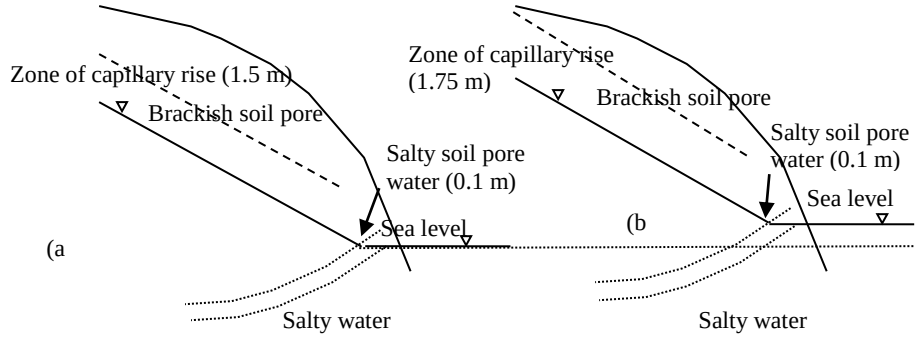

Figure 4.13 Illustration of prediction results in year 2100 (a) under stationary sea level and (b) under 1 m sea level rise

4.5.3 Flood with stationary sea level

When the temperature is increased, the evaporation may increase. Some countries at the equator and the tropical zone may suffer with flooding. The prediction indicates more than 10% of currently rainfall intensity may be increased. The simulation was employed using the same input data as presented in laboratory scale, only the domain was increased to be 500 cm. The seawater movement was indicated by the distributions of pressure head and volumetric water content. The simulations are presented in Figure 4.14. However, the heavy rainfall could push the saltwater via the gravitational force of massive inflow water. According to the pressure head distribution, the sand pores at the elevations 0-120 cm were full with seawater. Above this elevation till 430 cm, the capillary force could withdraw the seawater and freshwater, this could be accounted as the mixing zone. Beneath the column surface to the elevation of 430 cm, the freshwater was filled into the sand pore. Based on the distribution of volumetric water content, the intermediated zone was at the elevations of 0-120 cm above the datum. The capillary could bring the seawater to mix with freshwater at the elevations of 120-430 cm above the datum. The freshwater was filled in the soil pore at the elevations of 430-500 cm above the datum.

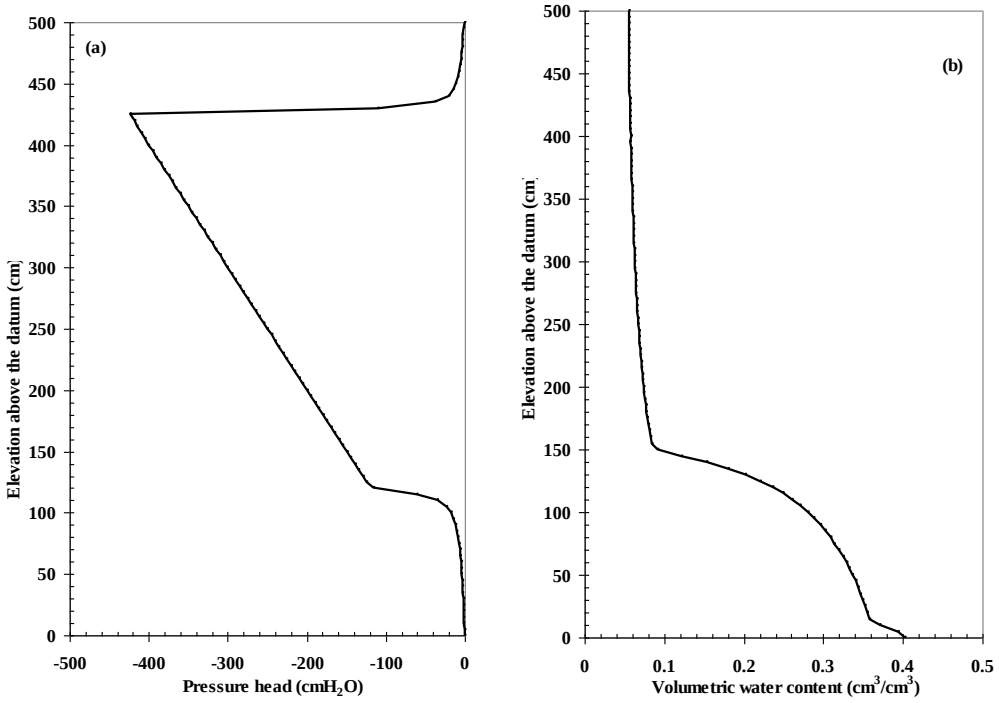

Figure 4.14 Simulation of seawater movement at coastal sandy aquifer (a) pressure head distribution and (b) volumetric water content distribution under flood with stationary sea level

The massive infiltration can dilute and flush the NaCl, the sand pore water contains no NaCl. The simulation results are presented in Figure 4.15. The capillary rise can abstract the saltwater to the elevations of 175 and 120 cm in cases of drought and flood, respectively. This could indicate that the capillary force can abstract the seawater in case of drought. However, the heavy rainfall could push the saltwater via the gravitational force of massive inflow water. Under the drought condition, the NaCl can contaminate the freshwater at the pores of sand. The sand porewater becomes brackish water along the sandy aquifer. On the other hand, the massive infiltration can dilute and flush the NaCl, the sand pore water contains no NaCl. The interface between salt and fresh water was observed at the elevation of 0.10 m for both conditions, but the magnitude of NaCl contamination was less when the flood was taken placed.

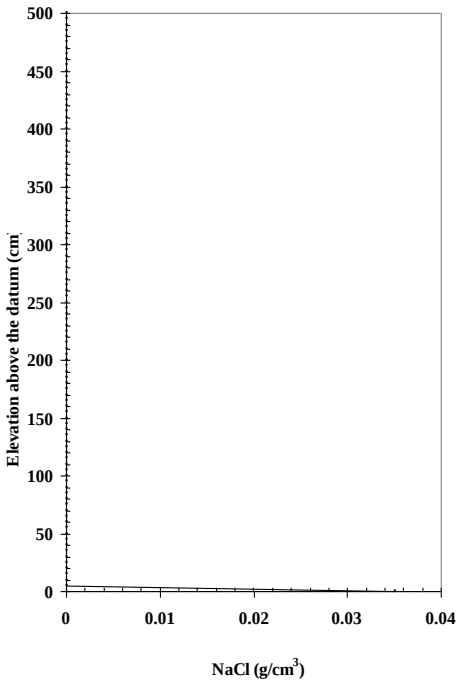

Figure 4.15 Simulation of NaCl concentration profile at coastal sandy aquifer under flood with stationary sea level

Figure 4.16 describes the pattern of seawater movement when the area was either flood or drought, with stationary sea level. This could overview the effect of flood and drought onto the migration of salt towards the land. As same as the simulation of laboratory scale sand column, the accumulated NaCl may be washed out the sand pore, when the heavy rainfall was occurred. However, the NaCl at the intermediated zone between water table and capillary zone was diluted when the heavy rainfall was applied. The sand porewater at this zone becomes brackish water. However, the capillary force could influence the brackish water move upwards. The freshwater applied at the surface then flowed gravitationally, it could mix with the brackish water at the capillary zone. Hence, the low salinity water may be occupied at the capillary zone. The amount of availability of freshwater at the coastal aquifer may be high, when there was heavy rainfall.

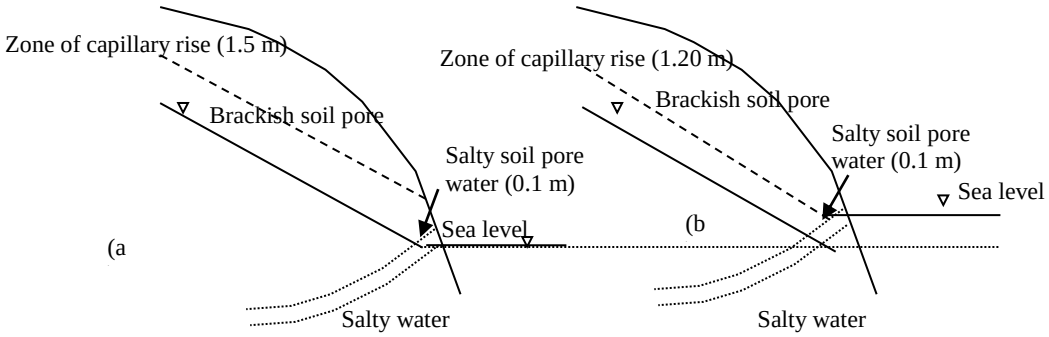

Figure 4.16 Illustration of prediction results in year 2100 (a) flood and (b) drought with stationary sea level

According to the simulation, the constants are obtained as shown in Table 4.11. The same statement were presented as the laboratory scale sand column test, the seawater could penetrate the unsaturated zone rapidly, when it was drought with sea level rise. The volumetric moisture content of sand was increased due to the filling seawater. In case of flooding, the freshwater could be mixed with saltwater and the flume of slightly concentrated NaCl may present in the large area. This could suggest that the NaCl could less contaminate the unsaturated sand layer, when there was flood with stationary sea level.

Table 4.11 Constants for seawater movement in unsaturated sand layer in Thailand Gulf

Parameter	**Unsaturated sand layer with**		
	Drought and stationary sea level	**Drought and sea level rise**	**Flood and stationary sea level**
Darcy's velocity (cm/h)	-0.0056	-0.0154	-0.0189
Averaged volumetric moisture content (cm^3/cm^3)	0.1485	0.1729	0.1633
NaCl dispersion coefficient (cm^2/h)	0.0370	0.0635	0.0802

4.6 Soil column tests

In the same manner, the UNSAT model was calibrated with the laboratory scale silt column to determine the specific boundary conditions for three serious environmental conditions, e.g. drought with stationary sea level, drought with sea level rise and flood with stationary sea level. The details of calibration results were presented as follows.

4.6.1 Drought with stationary sea level

The input parameters for seawater movement in unsaturated silt layer are given in Table 4.12. The hydraulic pressure head at the column surface was slightly lower than the sand column test. The capillary rise along the silt layer was lower than the sand layer as the particles of silt was looser than sand layer, the particles of silt could be swallow when the pores were filled with seawater. Hence, the expansion of silt layer was observed and it could block the water to move upwards.

Table 4.12 Inputs for seawater movement under drought with stationary sea level

Parameter	Values
Domain	20 cm thick silt layer
Total considered period	1 hour
Number of time step	120
Hydraulic properties model	van Genuchten (constants are in Table 4.3)
Boundaries condition	Hydraulic pressure head at the surface and the base of column were -20.0 and 0 cmH_2O, respectively.

The simulation results for distributions of pressure head and volumetric water content are illustrated in Figure 4.17. The linear distribution of pressure head was obtained. This could suggest that the seawater could upwards flow due to capillary force. The whole layer of silt was full with sea water. This could make the serious problem of amount of available freshwater inside the silt pore. The silt particles could highly absorb and hold the seawater for a longer time. The creep of seawater was relatively slow after the silt layer was full saturated with seawater. The distribution of volumetric moisture content was presented as the straight line, which was closed to the fully saturated volumetric moisture content.

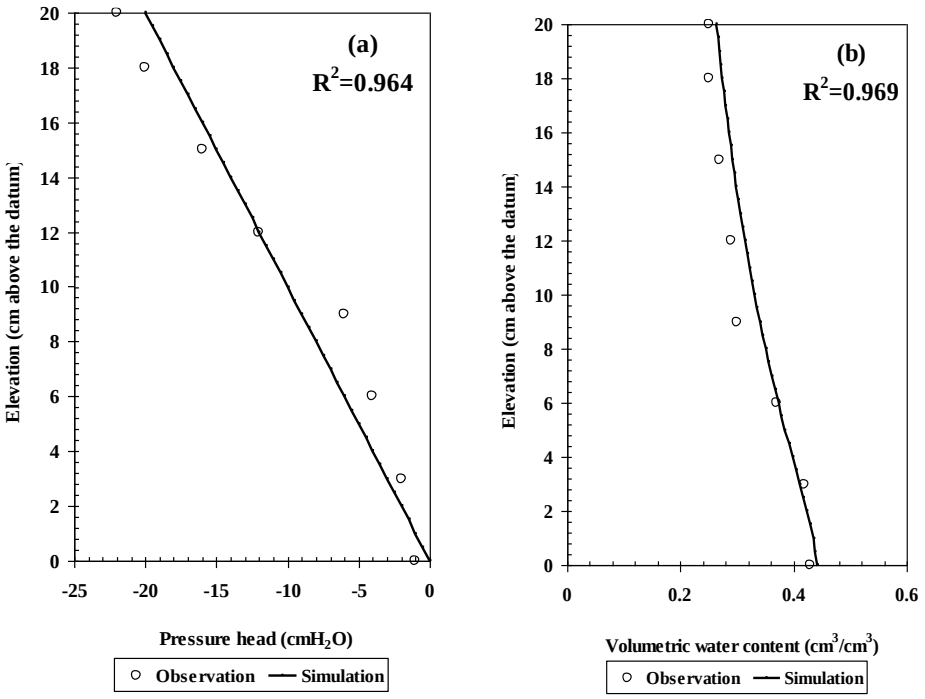

Figure 4.17 Distributions of (a) pressure head and (b) volumetric water content at unsaturated silt layer under drought with stationary sea level

With highly concentrated NaCl inside the pores, the NaCl may be deposited and becomes the salt rock. Besides, the small pore of silt could be enlarged, retarding an enormous of seawater. The simulation of NaCl concentration profile was further undertaken. The input parameters are provided in Table 4.13.

Table 4.13 Inputs for NaCl distribution under drought with stationary sea level

Parameter	Values
Domain	20 cm thick silt layer
Total considered period	1 hour
Number of time step	120
Boundaries condition	The concentration of NaCl at the column base is 35 g/L. The initial concentration of NaCl is 14.46 g/L.
Molecular diffusion	0.04788 cm^2/h

The simulation of NaCl concentration profile is presented in Figure 4.18. The NaCl concentration profile described that the seawater could contaminant the silt particle, the porewater inside the column was full with NaCl. However, the high background

concentration of NaCl of silt could slow down the molecular diffusion process. The whole layer of silt was acknowledged as the salty aquifer.

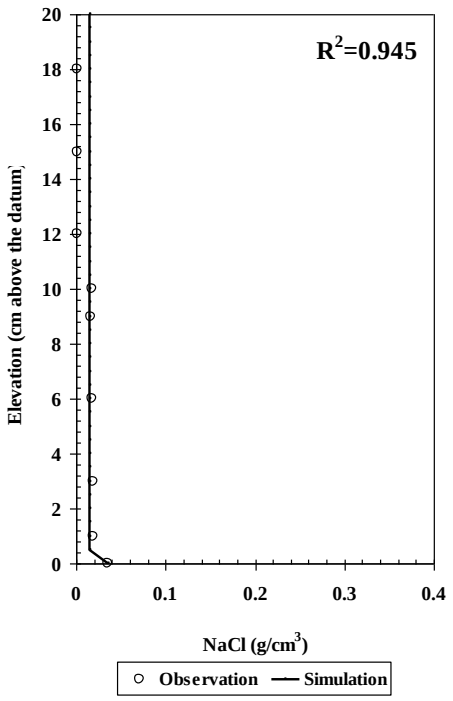

Figure 4.18 Distribution of NaCl at unsaturated silt layer under drought with stationary sea level

4.6.2 Drought with sea level rise

The simulation of seawater movement in silt layer under drought with sea level rise was employed. The input parameters are presented in Table 4.14. Only the pressure head applied at the column base was increased to 2 cmH_2O. Figure 4.19 explains the distribution of pressure head and volumetric water content of unsaturated silt layer.

Table 4.14 Inputs for seawater movement under drought with sea level rise

Parameter	Values
Domain	20 cm thick silt layer
Total considered period	1 hour
Number of time step	120
Hydraulic properties model	van Genuchten (constants are in Table 4.3)
Boundaries condition	Hydraulic pressure head at the surface and the base of column were -20.0 and 2.00 cmH_2O, respectively.

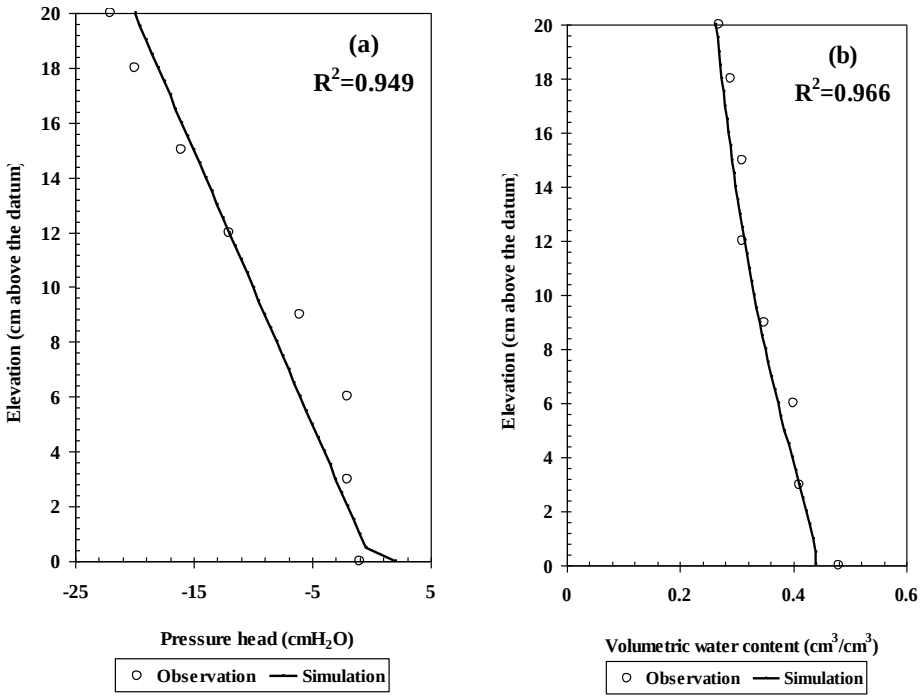

Figure 4.19 Distributions of (a) pressure head and (b) volumetric water content at unsaturated silt layer under drought with sea level rise

The distributions of pressure head and volumetric water content had indicated that the increasing of level of seawater did not much affect the column, as the column was saturated with seawater. The distribution of pressure head was linear, only the pressure head at first 2 cm above the datum was increased due to rising of elevation head. The distribution of volumetric moisture content looked like the straight line, closing the fully saturated volumetric water content.

The inputs for simulation of NaCl concentration profile is presented in Table 4.15. The simulation result is expressed in Figure 4.20. The same input were inserted only the different boundaries condition for seawater movement was retrieved from previous simulation. As the seawater movement under drought with sea level rise was slightly different from the one with drought and stationary sea level, the observation was undertaken at the equilibrium of inflow and outflow. The column was fully saturated, hence the concentration profile of NaCl for this simulation was same as previous case. This could confirmed that the sea level rise did not affect the quality of porewater as it was naturally filled with seawater and eventually became the salty aquifer.

Table 4.15 Inputs for NaCl distribution under drought with sea level rise

Parameter	Values
Domain	20 cm thick silt layer
Total considered period	1 hour
Number of time step	120
Boundaries condition	The concentration of NaCl at the column base is 35 g/L. The initial concentration of NaCl is 14.46 g/L.
Molecular diffusion	0.04788 cm^2/h

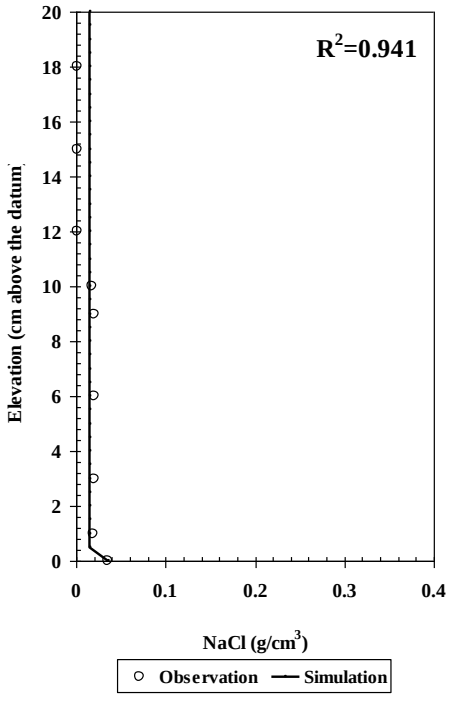

Figure 4.20 Distribution of NaCl at unsaturated silt layer under drought with sea level rise

4.6.3 Flood with stationary sea level

The simulation for seawater movement under flood with stationary sea level rise was done to compare whether the pattern of seawater could be influenced by flooding. The input parameters are presented in Table 4.16. The simulation results are provided in Figure 4.21. The input for seawater movement was obtained by assuming the silt layer at the top was fully saturated with freshwater and the silt layer at the base was also full with seawater. Hence, the pressure heads at elevations of 0 and 20 cm above the datum became 0 cmH_2O. The distribution of pressure head had shown that the whole column was full with either seawater or freshwater. The distribution of volumetric water content described the same statement as the distribution of pressure head. The straight line of volumetric water distribution was yielded. It could believe that the under flood with stationary sea level, the silt layer was under fully saturated condition.

Table 4.16 Inputs for seawater movement under drought with sea level rise

Parameter	Values
Domain	20 cm thick sand layer
Total considered period	1 hour
Number of time step	120
Hydraulic properties model	van Genuchten (constants are in Table 4.3)
Boundaries condition	Hydraulic pressure head at the surface and the base of column were 0.00 and 0.00 cmH_2O, respectively.

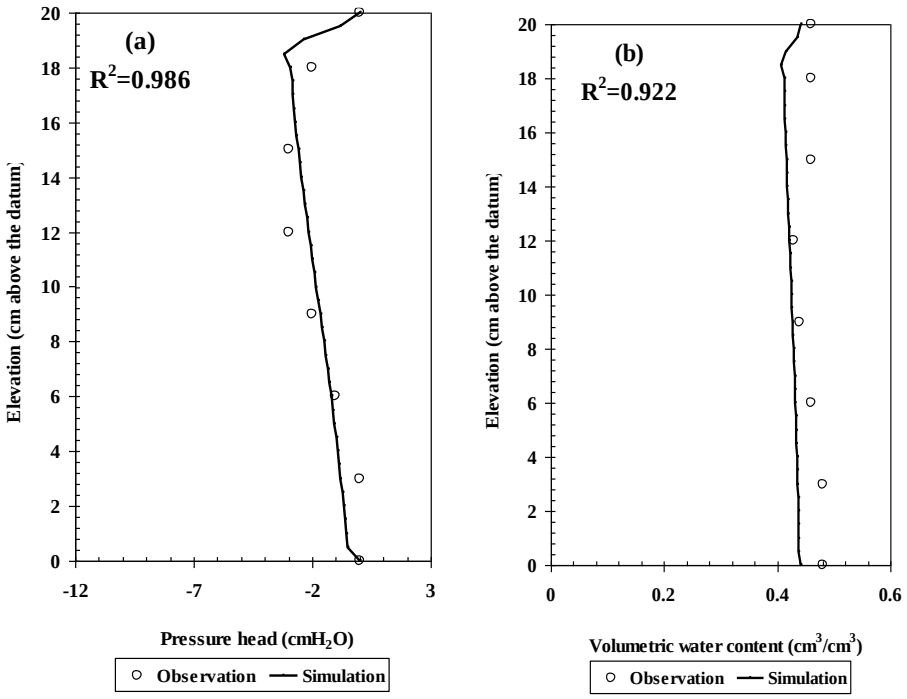

Figure 4.21 Distributions of (a) pressure head and (b) volumetric water content at unsaturated silt layer under flood with stationary sea level

To be ensured that the column was contaminated with seawater or it was filled with freshwater, the set of input data are placed into UNSAT program. The input parameters were same as previous case, accepting the freshwater with salinity at 0 g/L was applied on the column surface. The input parameters are in Table 4.17 and the simulation is expressed in Figure 4.22.

Table 4.17 Inputs for NaCl distribution under flood with stationary sea level

Parameter	Values
Domain	20 cm thick silt layer
Total considered period	1 hour
Number of time step	120
Boundaries condition	The concentration of NaCl at the column base is 35 g/L. The initial concentration of NaCl is 14.46 g/L. The concentration of NaCl at the surface is 0 g/L.
Molecular diffusion	0.04788 cm^2/h

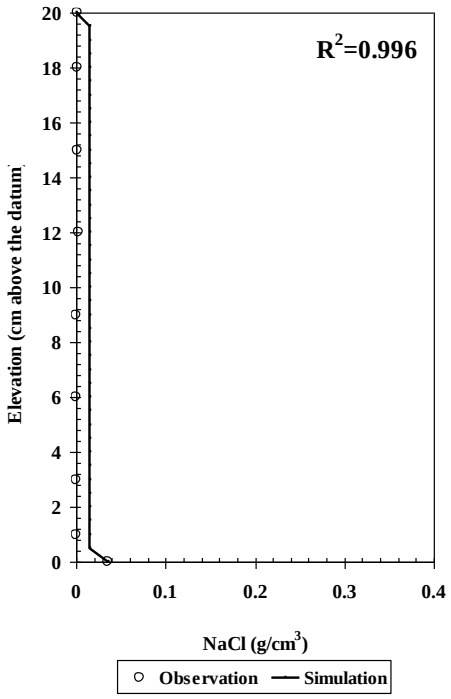

Figure 4.22 Distribution of NaCl at unsaturated silt layer under flood with stationary sea level

The simulation of NaCl concentration distribution could inform that the freshwater could either diluting or flushing the seawater. The NaCl content of silt layer was slightly reduced. The freshwater could not completely remove the NaCl from pore. The high background NaCl concentration of silt could not been beat by adding this amount of freshwater.

The constants yielded from simulations such as Darcy's velocity, averaged volumetric water content and dispersion coefficient are presented in Table 4.18. Under drought with sea level rise, the seawater could move quickly through silt layer rather than another with stationary sea level. The elevation head could influence the upwards movement the seawater. The more amount of seawater could fill the pore of silt under drought with sea level rise than the drought with stationary sea level. The dispersion coefficients for drought with stationary sea level and with sea level rise were insignificantly different. This referred that the seawater filled inside the pore became saturated hence there was no molecular diffusion. The influence of flood on sweater movement was obviously found, Darcy's velocity of freshwater was high and the porewater became slightly salt water. The NaCl diffusion coefficient was the largest as

the molecular diffusion was increased. The freshwater could dilute and flush the seawater. The silt layer could less suffer from NaCl contamination. The same statement could be made that the sea level did less affect to the seawater movement, but the change of hydrological cycle in particular drought and flood could highly influence the movement of seawater upwards to unsaturated silt aquifer.

Table 4.18 Constants for seawater movement in unsaturated silt layer

Parameter	Unsaturated silt layer with		
	Drought and stationary sea level	**Drought and sea level rise**	**Flood and stationary sea level**
Darcy's velocity (cm/h)	-0.00036	-0.00042	-0.00238
Averaged volumetric moisture content (cm^3/cm^3)	0.3489	0.3586	0.4135
NaCl dispersion coefficient (cm^2/h)	0.0148	0.0150	0.1600

4.7 Model applications for silty aquifer

The UNSAT program was further applied to simulate the seawater movement at silty aquifer. The case study was at the mangrove forest in Phetchaburi, Thailand. The unsaturated zone of aquifer at this area was only 1.5 m deep and it was classified as silty aquifer. The critical environmental conditions were applied such as drought with stationary sea level, drought with sea level rise and flood with stationary sea level. The boundaries conditions yielded from the model calibration process were input to this case study. The results were expressed as follows.

4.7.1 Drought with stationary sea level

The input and boundaries condition applied to this case study was same as the part of model calibration, only the thickness of silt layer was extended to 1.5 m. The hydrological condition applied was the same as the case study for sandy aquifer at Thailand Gulf. As the Phetchaburi is located at the same latitude and longitude as

Thailand Gulf, the hydrological conditions are same. The simulations of distributions of pressure head and volumetric water content are in Figure 4.23.

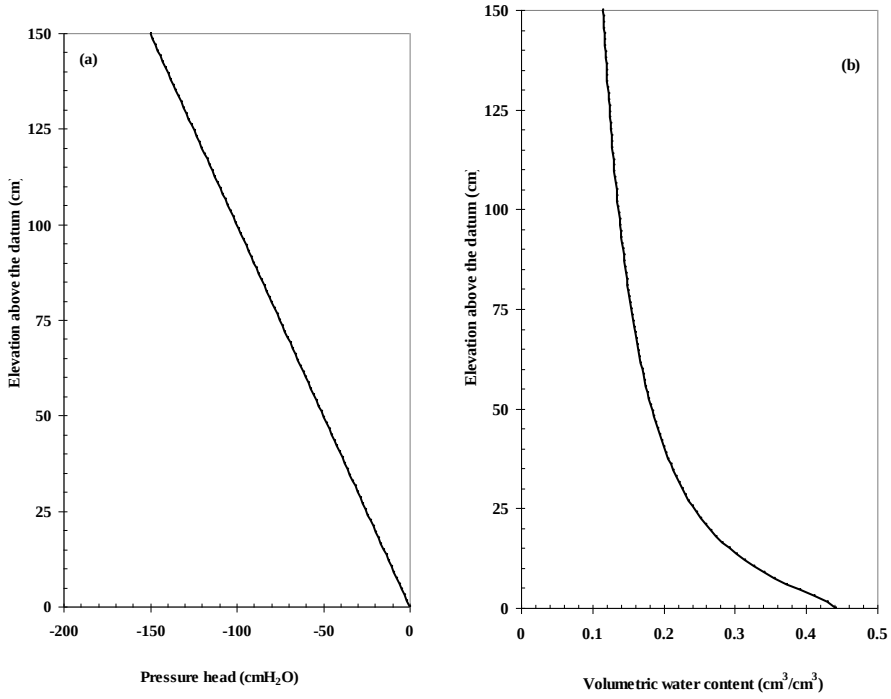

Figure 4.23 Simulation of seawater movement at coastal silty aquifer (a) pressure head distribution and (b) volumetric water content distribution under drought with stationary sea level

The simulation results for distributions of pressure head indicated that the seawater could upwards flow dealing with the capillary force. The linear distribution of pressure head was obtained. The distribution of volumetric content suggested that the silty aquifer at the elevations of 0-25 cm above the datum was contaminated with seawater. The porewater at portion above this elevation may be turned to be brackish water. With the same boundary contained governed from the model calibration, the distribution of NaCl concentration in unsaturated silty layer was undertaken. The simulation result for distribution of NaCl in unsaturated silt layer is presented in Figure 4.24.

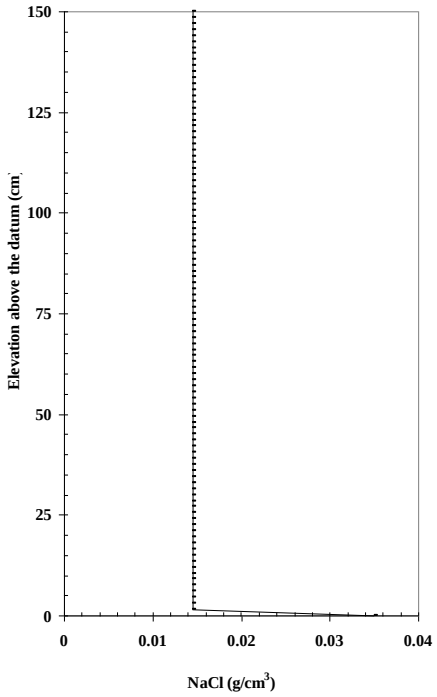

Figure 4.24 Simulation of NaCl concentration profile at coastal silty aquifer under drought with stationary sea level

The simulation for NaCl distribution claimed that only 2.5 cm of silt aquifer above the sea level was affected. The pore was full with seawater. The remaining portion above this elevation was filled with brackish water. This could be recognised as the self protection as the permeability of silty aquifer was very low. The movement of seawater upwards may take a long time. When silty aquifer was saturated with seawater or full with brackish water, the flux of upflows seawater may be constant. There was no more salt intrusion. The mangrove forest could be served with porewater at constant NaCl content. Besides, the marine ecological may be less disturbed since the content of NaCl in porewater was stagnant at 14.5 g/L.

4.7.2 Drought with sea level rise

The simulations for pressure head and volumetric water content distributions are presented in Figure 4.25. The simulations were obtained by inserting the set of input data and the specified boundary conditions presented in the model calibration process. The sea level rise could carry some amount of seawater to the elevation of 0-50 cm above the datum. The thickness of unsaturated zone was reduced to 1.0 m. The distribution of pressure head at the elevation 50-100 cm above the datum was still

linearly. The capillary could abstract some amounts of sweater and accumulated inside the pore. Based on the distribution of moisture content, the saturation zone was risen up to the elevation of 50 cm above the datum. The seawater could move upwards due to the capillary force.

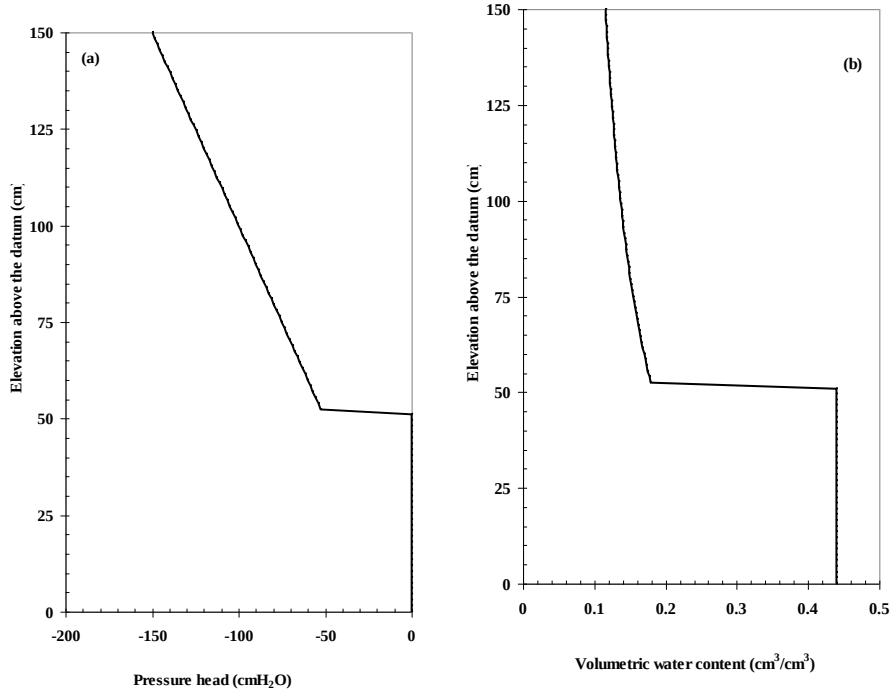

Figure 4.25 Simulation of seawater movement at coastal silty aquifer (a) pressure head distribution and (b) volumetric water content distribution under drought with sea level rise

The simulation of NaCl concentration profile was conducted using the input and boundary conditions yielded from the model calibration. The simulation result is provided in Figure 4.26. The silt layer at the elevation 0-50 cm above the datum was full with seawater. The unsaturated zone above this layer was contaminated with seawater. A 2.5 cm of silt thickness at the elevation of 50-52.5 cm was full with seawater. Apart from this portion, the brackish water was filled inside the pore. This silty aquifer was accounted as the brackish aquifer. This simulation could confirm that the self protection of the silty aquifer was effective and active. The low permeability of silty aquifer could hold the seawater and make the equilibrium of inflow and outflow system. Hence, the NaCl content in the porewater was constant at the level of 14.5 g/L. The marine ecological cycle may be less affected as the NaCl content in the porewater was maintained by this natural mechanism.

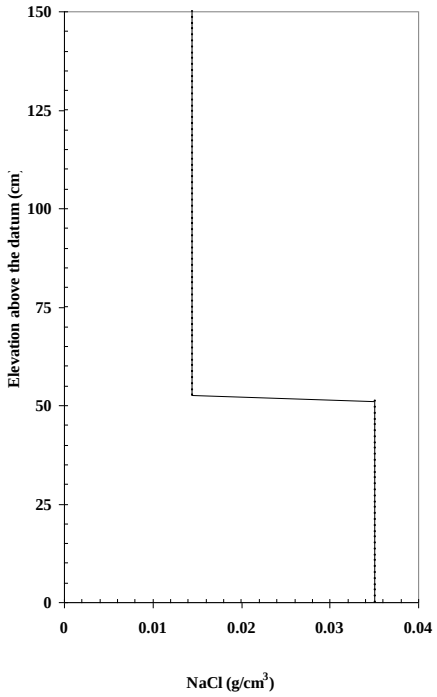

Figure 4.26 Simulation of NaCl concentration profile at coastal silty aquifer under drought with sea level rise

To overview the influence of sea level rise on availability of groundwater at the mangrove forest in this considered area. The simulations from drought with stationary sea level and sea level rise are compared as shown in Figure 4.27. The water table at the aquifer may be raised for 1.0 m, after an increasing of a metre of seawater. The porewater was turned to be salty water. The available water was reduced. However, the whole unsaturated layer was full with the brackish water. Both cases suggested that the sea level less disturbed the NaCl content in the pore, as the low permeability of silt aquifer could naturally maintain the equilibrium of inflow and outflow.

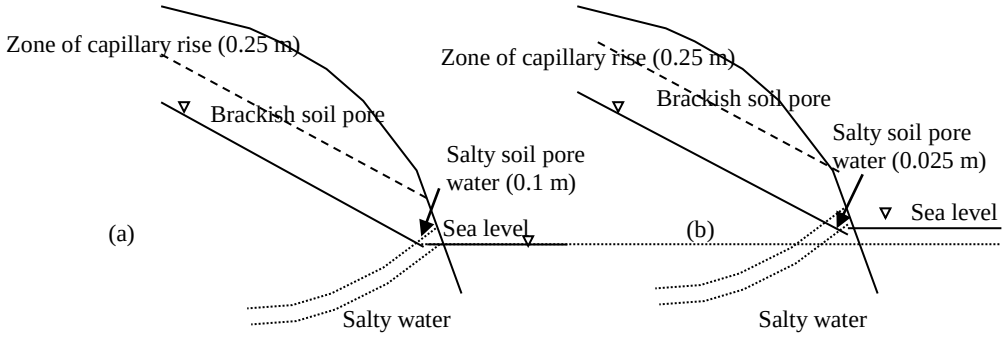

Figure 4.27 Illustration of prediction results in year 2100 (a) under stationary sea level and (b) under 1 m sea level rise

4.7.3 Flood with stationary sea level

The simulations for sweater movement in unsaturated zone at the mangrove forest, were employed by inputting the constants and boundaries condition obtained from the model calibration process. The heavy rainfall infiltration rate was applied as the same manner as the previous case study of costal aquifer. The distributions of pressure head and volumetric water content are illustrated in Figure 4.28. The distribution of pressure head suggested that the lower portion of unsaturated zone at elevation of 0-25 cm above the datum was fully saturated with seawater. The unsaturated layer at the elevations between 25 cm and 135 cm above the datum was partially full with seawater. The unsaturated layer at the elevations 135 to the surface was partially filled with the infiltration water. However the permeability of silt was very low, the infiltration may gradually percolate from the surface to the deeper layer. This process could consume very long period. Therefore, the washing of salty aquifer and the salt extrusion may not be observed within the short period. The distribution of volumetric water content showed the same statement as the distribution of pressure head. The unsaturated zone at the elevations of 0-25 cm above the datum was full with saltwater and the unsaturated layer at the elevations of 25-135 cm above the datum was relatively dried. At the elevations of 135 cm above the datum until the surface, the infiltration could reach, resulting in the gravitational flow region.

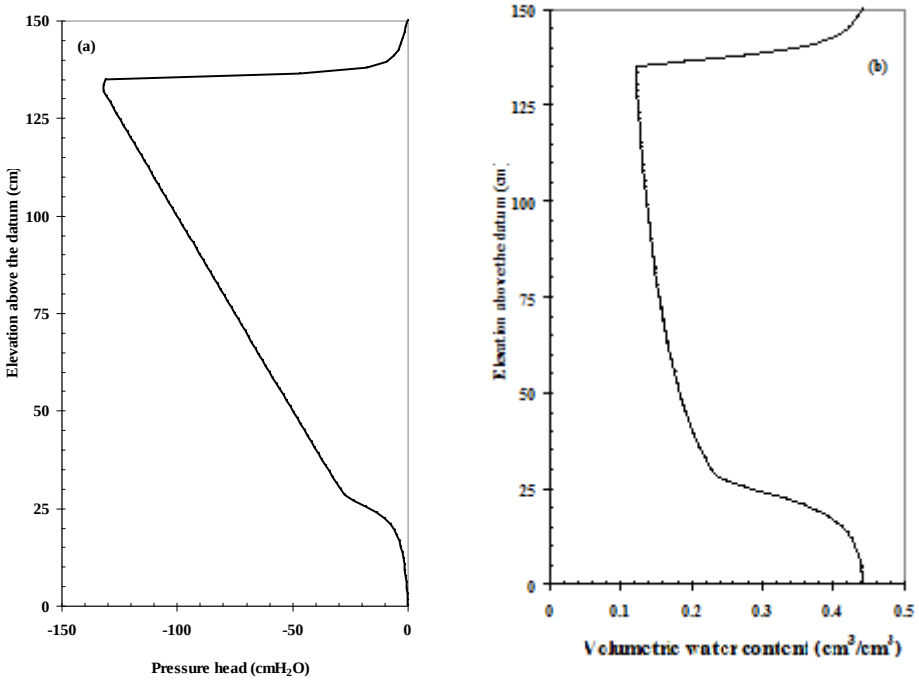

Figure 4.28 Simulation of seawater movement at coastal silty aquifer (a) pressure head distribution and (b) volumetric water content distribution under flood with stationary sea level

The simulation for NaCl concentration profile is presented in Figure 4.29. The infiltration water with NaCl concentration of 0 g/L was applied to the surface of silty aquifer. The infiltration could replace the saltwater for only few centrimetres. The thin layer of freshwater stayed on the top of brackish water. As the density of freshwater was lower than the brackish and seawater, the freshwater may difficultly percolate or replace the brackish water layer. The seawater was contaminated the aquifer a few centrimetre at the lower layer above the sea level. The buffer zone, which was partially dried unsaturated layer could not only prohibit the movement of seawater into aquifer, but also prevent the downwards movement of freshwater. The mixing between freshwater and seawater was very low. There was no dilution effect in the porewater. The salinity level of porewater was constant at 14.5 gNaCl/L. In this case study, the natural properties of silty aquifer could prevent the change of salinity level in the porewater. The marine ecological system may not face the serious impact from changing of climatic conditions.

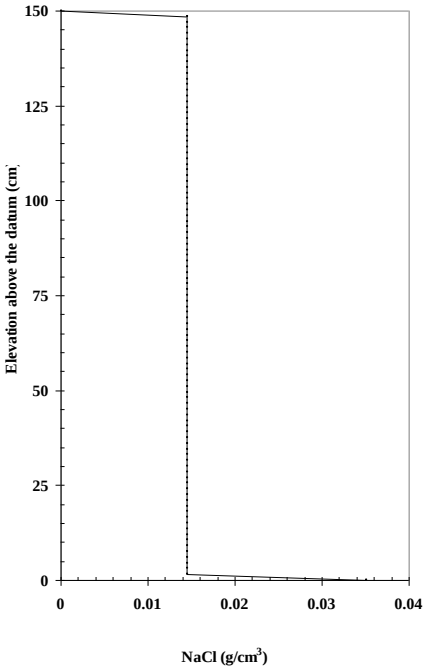

Figure 4.29 Simulation of NaCl concentration profile at coastal silty aquifer under flood with stationary sea level

The effect of shifting of hydrological cycle onto the salinity level of porewater at the silty aquifer was simplified as illustrated in Figure 4.30.

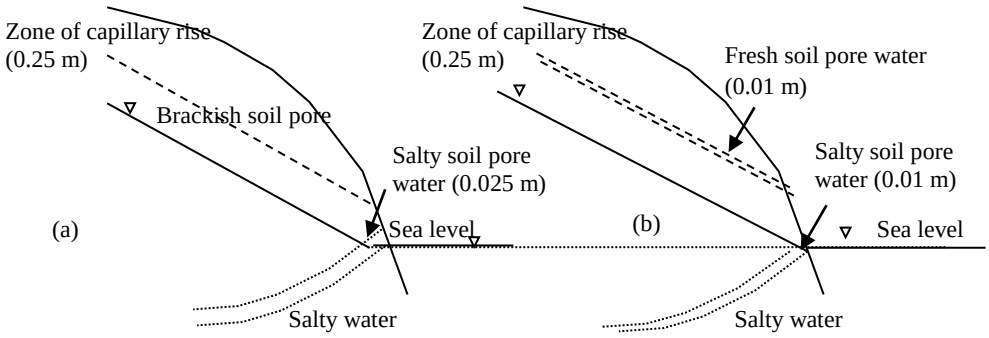

Figure 4.30 Illustration of prediction results in year 2100 (a) under drought and (b) under flood with stationary sea level

The constants yielded from model applications at various environmental conditions are given in Table 4.19.

Table 4.19 Constants for seawater movement in unsaturated silt layer in mangrove forest at Phetchaburi, Thailand

Parameter	Unsaturated silt layer with		
	Drought and stationary sea level	**Drought and sea level rise**	**Flood and stationary sea level**
Darcy's velocity (cm/h)	-0.00058	-0.00074	-0.00872
Averaged volumetric moisture content (cm^3/cm^3)	0.3852	0.3926	0.4211
NaCl dispersion coefficient (cm^2/h)	0.0192	0.0263	0.6895

The obtained constants indicated that the sea level could less influence the upwards flow of seawater. The aquifer could response the increasing of sea level by naturally retardation of upwards flow. The low permeability of silt aquifer could maintain the equilibrium of inflow and outflow. Even though the elevation head was increased for 1 m after sea level was raised, the low permeability could prohibit the upwards movement of seawater. The values for Darcy's velocity, averaged volumetric water content and NaCl dispersion coefficient from the case of drought with sea level rise were slightly higher than the case of drought with stationary sea level. Furthermore, the shifting of hydrological cycle seemed to highly influence the quantity and quality of porewater. The seawater could move downwards with a relatively high velocity when there was flooding. The freshwater could gradually percolate and replace the seawater, however it took a long period. The silt particles could be relatively wet, when there was flooding. The averaged volumetric water content was closed to the fully saturation level. There were small amount of freshwater inside the pore. The NaCl diffusion was highly obtained as the diffusion seawater could be driven be the molecular flux. The flume of saltwater could be expanded horizontally to some distance.

CHAPTER 5 CONCLUSIONS AND RECOMMENDATION

5.1 General approaches

This research focused on the perdition of saltwater intrusion, extrusion in the coastal area for forecast the occurring of brackish water in the mangrove forest. The considered case studies were located at the sensitive areas. They were the sandy aquifer at the coastal area of Thailand Gulf and the silty aquifer at the mangrove forest, Phetchaburi, Thailand. Both areas were located at the equator and they were recognised as the tropical zone. Based on the IPCC report and literatures, the tropical zone may face with rapidly changes of environmental conditions, particular the shifting of hydrological cycles and fluctuating of sea level. The atmospheric model could project the weather condition in year 2100. The simulation had shown that the rainfall intensity may either be declined by 10-25% from the present or be increased by 13-18% by the present, these could bring either drought or flood, respectively. Furthermore, the sea level may possibly oscillate between 0.11 and 0.88 m from the present or constant at the same level as present. Since no single simulation could represent the situation in the year 2100, the impacts of climate change on availability of water would be challenged to be predicted. The worse scenarios were assumed including of drought with stationary sea level, drought with sea level rise and flood with stationary sea level. These environmental conditions were applied to UNSAT program to evaluate the movement of seawater and the distribution of NaCl in the soil pore at the unsaturated zone. The porewater at unsaturated zone could be available for some purposes such as water supply from shallow well and agriculture. Besides, the amount of porewater at unsaturated zone was preserved for salt intrusion and it could maintain the costal ecological system as well as coastal wetland.

5.2 Specific approaches

The UNSAT program was calibrated with the laboratory scale sand and silt columns to identify the constants for hydraulic properties model and pattern of seawater movement. The river sand and silt with particle size between 200 and 500 μm, were packed into a 6.5 cm diameter and a 20 cm deep column to simulate the homogenous sandy and silty unconfined aquifer. The tests were operated with three conditions, which were drought (infiltration rate was 0 cm_3/d) with stationary sea level (level of seawater in the tank was

maintained at 0 cm above the datum), drought with sea level rise (level of seawater was at 2 cm above the datum), and flood (infiltration rate was 80 cm^3/d) with stationary sea level. The simulations indicated that the sandy aquifer may highly suffer with salt intrusion, where there were under drought with stationary sea level and with sea level rise. The seawater could move upwards to the elevations of 12, 10 and 1cm above the datum, when the sand columns were under drought with stationary sea level, drought with sea level rise and flood with stationary sea level, respectively. Besides, the infiltration could be cumulated at sand layer for 2 cm thick. The NaCl content of sand layer for every tests at the elevation of 1 cm was closed to 35 g/L, confirming the porewater was salty. Above this thin layer, the porewater was turned to be brackish water. For silt columns test, the seawater could flow upwards to whole columns for every test. A 0.3 cm thick of silt layer above the seawater level was full with salty water. Apart from this thin strip, the porewater was classified as brackish water.

The input and boundary conditions were employed to the case studies, which were sandy aquifer at Thailand Gulf and silty aquifer in mangrove forest at Phetchaburi, Thailand. The simulations for seawater movement in unsaturated zone at coastal sandy aquifer indicated that the aquifer may suffer from salt intrusion, when it was under drought with either stationary sea level or with sea level rise. The seawater could move upwards to the elevations of 180, 150 and 110 cm above the column, when the aquifer was under drought with stationary sea level, drought with sea level rise and flood with stationary sea level. The upflow of seawater was replied on the capillary force, which can abstract the seawater along the tiny pore of sand. The freshwater from infiltration could replace the seawater, a 0.7 m deep layer of soil pore at the top portion was full with freshwater. So, the costal aquifer at Thailand Gulf may suffer when there was drought with stationary sea level. The plume of seawater could be highly expand when there was flooding, so too the sand pore could be washed and the seawater could be diluted. This could increase the amount of available freshwater at the unsaturated zone. The shifting of hydrological cycle could bring the rapid change in both quantity and quality of groundwater at sandy aquifer in Thailand Gulf rather than the fluctuating sea level.

In case of silty unconfined aquifer in mangrove forest at Phetchaburi, Thailand, the same statement was obtained. The seawater could contaminated the porewater up to the

elevations of 25, 52.5 and 25 cm above the datum, when it was under drought with stationary sea level, drought with sea level rise and flood with stationary sea level, respectively. Only 2.5, 52.5 and 2.5 cm of silt layer at the lower portion closed to seawater table was full with saltwater, when it was drought with stationary sea level, drought with sea level rise and flood with stationary sea level, respectively. The freshwater from infiltration may be observed as a thin film with 2.5 cm thick at the surface of aquifer. The silty aquifer had a relatively low permeability, the equilibrium of inflow and outflow could be maintained for a long period, even the seriously environmental condition was applied. The magnitude of salt intrusion and extrusion was insignificantly observed. The level of NaCl content in pore was preserved at 14.5 g/L, which was brackish water. The marine ecological system particularly the mangrove forest could be survived even the changes of hydrological cycle and sea level were occurred.

5.3 Recommendation

This research could evaluate the change of quantity and quality of porewater at costal aquifer at Thailand Gulf and Phetchaburi, Thailand. The UNSAT program could well calibrated with the observation data. However, the prediction results may not be accurate, if there were any changes of climatic condition scenarios. The recommendations for future research are made as follows.

1. The predictive data could be further applied for sustainable harvesting of water resource at the sensitive areas under changing of climatic condition, for constructing the artificial recharge system and for maintaining the marine ecological system.
2. The UNSAT program may be applied to determine the other impact of shifting of hydrological cycle under climate change, such as landslide and soil erosion.

REFERENCES

Adrian, D.W. and Craig, T.S., (2009), "Impact of sea-Level Rise on Sea Water Intrusion in Coastal Aquifers", **Ground water**, Vol. 47, pp. 197-204.

American Society for Testing and Materials International, ASTM. (1999). **Annual book of ASTM Standards**, Pennsylvania: ASTM international.

Arnell, N.W. (1999), **The effect of climate change on hydrological regimes in Europe: a continental perspective.** Global Environmental Change 9, pp 5-23.

Bear, J., and G. Dagan (1964), "Moving interface in coastal aquifers", **J. Hydraul. Div. Proc. Am.Soc. Civ. Eng.,** 90(HY4), pp. 193-216.

Bear, J., (1987). **Hydraulic of groundwater**, McGraw-Hill, ISBN 978-048-6453-552, New York, USA.

Bunsri, T., (2006), **Contaminant transport processes in onsite waste disposal system**, Ph.D. thesis, University of Wollongong.

Carsel, R. F. and Parrish, R. S. (1988), "Developing joint probability distributions of soil-water retention characteristics", **Water Resources Research** Vol. 24, No.5, pp. 755-769.

Demirel, Z. (2003), "The history and evaluation of saltwater intrusive into a coastal aquifer in mersin, Turkey**"**, **Journal of Environmental Management**, Vol. 70, pp. 275-282.

Elhassadi, A. (2007), "Sea water intrusion in Derna located in the Green mountain region, Libya- a threatening recurrent phenomenon calling for desalination", **Desalination**, Vol.220, pp. 189-193.

Gardner, W.H., (1965), "Water content", In **Methods of Soil Analysis**, Part 1 C.A Black(ed), Agronomy No.9. Am. Soc. Of Agron. Madison, Wisconsin, USA, pp.82-127.

Giambastiani, B.M.SS., Antonellini, M., Essink, G.H.P.O. and Stuurman, R.J. (2007), "Saltwater intrusion in the unconfined coastal aquifer of Ravenna (Italy**)**: A numerical model", **Journal of Hydrology**, Vol. 340, pp. 91-104.

Hanson, B., Grattan, S.R. and Fulton, A, (1999), **"Agricultural Salinity and Drainage."** University of California Irrigation Program, University of California, Davis.

Hardy, N., Shainberg, I, Gal, M. and Keren, R. . 1983, "The effect of water quality and storm sequence upon infiltration rate and crust formation", **Journal of Soil Science**. 34, pp. 665-676.

Henrry, H.R. (1960), **Salt intrusion into coastal aquifer**, Ph.D. thisis, Columbia University, New York.

Herzberg, B., 1901, Die Wasserversovgung einiger Nordseebaser, **J. Gasbeleucht and wasserversov**, Vol. 44, pp. 815-819.

Huyakorn, P.S., Thomas, S.D. and Thompson, B.M. (1984), "Technique for making finite element competitive in modeling flow in variably saturates porous media", **Water Resources Research**, Vol. 20, No. 8, pp. 1099-1115.

Intergovernmental Panel on Climate Change (IPCC), (1996), **Impacts adaptations and mitigation of climate change**: scientific-technicalanalysis.

Intergovernmental Panel on Climate Change (IPCC), (2001. **Climate change 2001**, The Scientific Basis, Cambridge University Press.

Intergovernmental Panel on Climate Change (IPCC), (2007), **Climate change 2007**, The Physical Science Basis, Cambridge: Cambridge University Press.

Jackson, M.L., (1967), **Soil Chemical analysis**, Prentice Hall of India Private Limited, New Delhi, p.498.

Kouzana, L., Mammou, A.B. and Felfoul, M.S (2007), **Seawater intrusion and associated processes: case of Korba aquifer**, Vol. 341, pp. 21-35.

Illangasekare, T., et al. (2006), "Impacts of the 2004 tsunami on groundwater resources in Sri Lanka", **Water Resour. Res**., Vol. 42, W05201.

Lookjan, A., Chalermyanont T. and Arrykul, S. (2009), "Three-dimensional density dependent seawater intrusion modeling for the Hat Yai basin", **The 14th National Convention on Civil Engineering**, Suranaree University of Technology, pp. 1253-1259.

Meteorological book, **Report of effected from climate**. Thai meteorological department, 2007.

Milnes, E. and Renard, P. (2003), "The problem of salt recycling and seawater intrusion in coastal irrigated plains: an example from the Kiti aquifer (Southern Cyprus)", **Journal of Hydrologgy**, Vol.288, pp. 327-343.

Misut, P.E., Schubert, C.E., Bova, R.G., and colabufo, S.R., (2003), **Simulated Effects of pumping and drought on Ground-Water Level and the Freshwater-Saltwater Interface on the North Fork, Long Island**, New York, U.S Geological survey Water Resource Investigations Report 03-4184.

Narayan, K. A., Schleeberger, C. and Bristow, K.L. (2007), "Modeling seawater intrusion in the Burdekin Delta irrigation area, North Queensland, Australia", **Agricultural Water Management**, Vol.89, pp. 217-228.

National Oceanic and Atmospheric Administration (NOAA). (1990), **Estuaries of the United States: Vital Statistics of a Natural Resource Base**. Rockville.

Nguyen, A.D., Savenije, H.H.G. and Pham, D.N. and Tang, D.T. (2007), "Using salt intrusion measurements to ddetermine the freshwater discharge distribution over the branches of a muti-channel estuary: The Mekong Delta case", **Estuarine coastal and shelf science**, Vol. 77, pp. 433-455.

Paulsen, R.J, O'Rouke, D, Smith, C.F and Wong, T.F., (2004), "Tidal Load and saltwater Inflluences on Submarine Ground Water discharge", **Ground Water**, Vol.42, No. 7, pp. 990-999.

Rhoades. J.D. (1977), "Potential for using saline agricultural drainage waters for irrigation", **Proceedings from Water Management for Irrigation and Drainage**, American Society of Civil Engineers. Reno, Nevada. July 20-22, 1977.

Shaw, R.J. (1999), "Soil salinity -electrical conductivity and chloride", In K.I. Peverill, L.A. Sparrow and D.J. Reuter (eds.), **Soil Analysis an Interpretation Manual**, Melbourne; CSIRO Publishing

Sheriff, J.M. and Singh, V.P. (1999), "Effect of climate change on sea water intrusion in coastal aquifers", **Hydrol. Proc**. Vol. 13, No.8, pp. 1277-1287.

Tiruneh, N.D. and Motz, L.H., (2003), **Three Dimensional Modeling of saltwater Intrusion Coupled with the Impact of Climate Change and Pumping**, World Water Environ. Resourc. Congr., ASCE, Philadelphia, pp. 1079-1087.

U.S Geological Survey (USGS) (2000), **Groundwater resources for the future-Atlantic Coastal Zone**, Fact Sheet 085-00, Reston, VA.

Urbano, L.D, (2001), **"The Impact of Climatic Change on Ground Water System"**, University of Minnesota

Van Genuchten, M. Th. (1980), "A closed-form equation for predicting the hydraulic conductivity of unsaturated soils", **Soil Science Society of America Journal**, Vol. 44, pp. 892-898.

Xu, C.Y. and Singh, V.P. (2004), "Review on regional water resources assessment models under stationary and changing climate", **Water Resources Management**, Vol. 18, pp. 591-612.

APPENDIX A

Physical and chemical properties of sand and soil

A.1 Physical properties of sand and soil

Table A.1 Soil particle size distribution and its classification

Test	Fraction (%)			Textural class
	Sand	**Silt**	**Clay**	
Sand				
1	96.89	3.11	0.00	Sand
2	97.12	2.88	0.00	Sand
Soil				
1	10.40	89.6	0.00	Silt
2	9.77	90.23	0.00	Silt

Table A.2 Bulk density

Test no.	**Type of sample**	**Bulk density (g/cm^3)**
1	**Sand**	2.57
2		2.58
3		2.55
Average		2.56
Test no.	**Type of sample**	**Bulk density (g/cm^3)**
1	**Soil**	1.11
2		1.11
3		1.11
Average		1.11

Table A.3 Specific Gravity of sand and soil

Test no.	Type of sample	Specific gravity
1	**Sand**	2.56
2		2.57
3		2.56
Average		2.56
Test no.	**Type of sample**	**Specific gravity**
1	**Soil**	1.20
2		1.22
3		1.20
Average		1.21

Table A.4 Water content and volumetric water content

Test no.	Type of sample	Water content (%)	Volumetric water content	Void ratio
1	**Sand**	1.02	1.75	0.37
2		1.00	1.75	0.37
3		1.04	1.75	0.37
Average		1.02	1.75	0.37
Test no.	**Type of sample**	**Water content (%)**	**Volumetric water content**	**Void ratio**
1	**Soil**	3.89	6.82	0.75
2		3.91	6.86	0.77
3		3.92	6.87	0.71
Average		3.90	6.85	0.74

Table A.5 Permeability

Test no.	Type of sample	Permeability (cm/sec)
1	**Sand**	0.0066
2		0.0071
3		0.0071
Average		0.0069
Test no.	**Type of sample**	**Permeability (cm/sec)**
1	**Soil**	0.0095
2		0.0091
3		0.0091
Average		0.0092

A.2 Chemical properties of sand and soil

Table A.6 Soil pH

Sample weight (g)	pH	Sample weight (g)	pH
Sand		Soil	
20.00	6.72	20.00	6.33
20.01	6.74	20.00	6.43
20.00	6.73	20.00	6.44
Average	6.73	**Average**	6.40

Table A.7 Conductivity and Salinity

Test no.	Type of sample	Sample weight (g)	Conductivity (µs/cm)	NaCl content (g/L)
1	**Sand**	20.00	42.00	0
2		20.00	37.60	0
3		20.00	41.20	0
Average		20.00	42.26	0
1	**Soil**	20.00	3667	1.50
2		20.00	3670	1.51
3		20.00	3667	1.48
Average		20.00	3668	1.50

APPENDIX B

Water retention curve of sand and soil

1. Water retention curve

Dimension of testing sand column:

Inner diameter 6.50 cm, Cross section area 33.2 cm^2, Total volume 199.00 cm^3, Sand specific gravity 2.56, The observation depth (from column base) 3.00 cm

Table B.1 Observation data of hydraulic properties in sand sample

Volume of water (cm^3)	**Sand weight (g)**	**Packing in bulk density (g/cm^3)**	**Moisture content (%)**	**Volumetric water content (%)**	**Pressure head (centibar)**	**Pressure head (cmH_2O)**
0	310.7	1.56	0.14	0.20	-10	-101.97
4	310.7	1.56	1.39	2.16	-10	-101.97
8	310.7	1.56	2.81	4.37	-9	-91.77
12	310.7	1.56	3.68	5.72	-9	-91.77
16	310.7	1.56	4.85	7.53	-8	-81.58
20	310.7	1.56	6.53	10.14	-7	-71.38
24	310.7	1.56	7.76	12.05	-7	-71.38
28	310.7	1.56	9.08	14.11	-5	-50.99
32	310.7	1.56	10.20	15.82	-5	-50.99
36	310.7	1.56	11.23	17.42	-4	-40.79
40	310.7	1.56	12.94	20.08	-3	-30.59
44	310.7	1.56	13.97	21.69	-3	-30.59
48	310.7	1.56	15.17	23.50	-2	-20.39
52	310.7	1.56	17.74	27.31	-2	-20.39
56	310.7	1.56	18.30	28.17	-2	-20.39
60	310.7	1.56	19.62	30.33	-1	-10.20
80	310.7	1.56	26.13	40.37	-1	-10.20
100	310.7	1.56	28.86	44.23	0	0

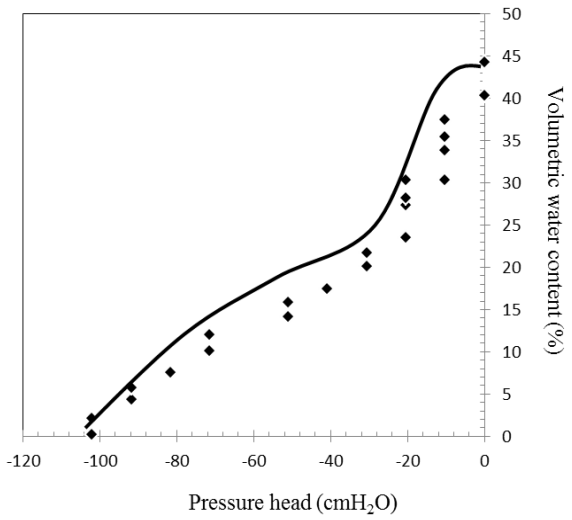

Figure B.1 Water retention curve of sand

van Genuchten hydraulic properties coefficients were determined. The mid point of water content; θ_p, was evaluated as follows.

$$\theta_p = \frac{\theta_S + \theta_r}{2}$$

The slope; *S* at point *p* was determined graphically from the experimental sand-water retention curve. The dimensionless slope; S_p was calculated graphically from the water retention curve.

$$S_p = \frac{S}{\theta_s - \theta_r}$$

The coefficient *m* was determined from the value of *Sp* with this given formula.

$m = 1 - \exp(-0.8 S_p)$ with $0 < S_p \leq 1$ or

$$m = \frac{0.5755}{S_p} + \frac{0.1}{S_p^2} + \frac{0.025}{S_p^3} \quad \text{with } S_p > 1$$

Then the coefficients, *p* and *a* were analysed by using the bubbling pressure. The equations were provided as follows.

$$p = \frac{1}{1-m} \text{ and } a = \frac{1}{h_b}(2^{1/m} - 1)^{1-m}$$

Determinations of hydraulic properties coefficients are given in Figure B.2.

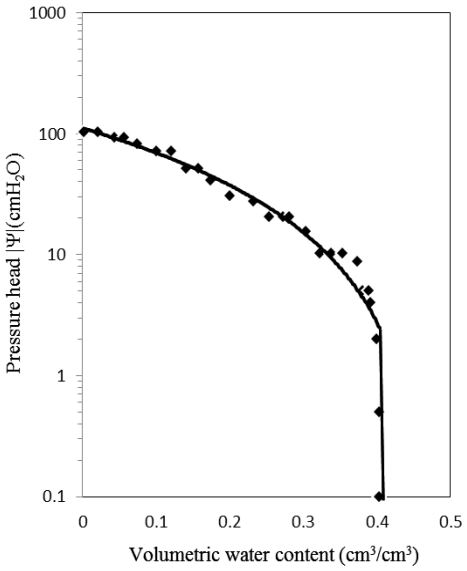

Figure B.2 Sand water retention curve

At the middle volumetric water content, θ_p , the slope of the curve, *S* is 0.144. The term *Sp* is 0.400. The bubbling pressure; log h_b is 1.560. The coefficients of *m*, *p* and *a* are 0.521, 2.080 and 0.045, respectively.

Dimension of testing soil column:

Inner diameter 6.50 cm, Cross section area 33.2 cm^2, Total volume 199.00 cm^3, Silt specific gravity 1.07, The observation depth (from column base) 3.00 cm

Table B.2 Observation data of hydraulic properties in silt sample

Volume of water (cm^3)	**Sand weight (g)**	**Packing in bulk density (g/cm^3)**	**Moisture content (%)**	**Volumetric water content (%)**	**Pressure head (centibar)**	**Pressure head (cmH_2O)**
0	58.5	0.32	4.94	1.45	-36	-367.092
2	58.5	0.32	8.59	2.51	-30	-305.91
4	58.5	0.32	11.87	3.46	-22	-224.334
8	58.5	0.32	19.44	5.67	-18	-183.546
12	58.5	0.32	25.64	7.48	-14	-142.758
16	58.5	0.32	32.75	9.53	-12	-122.364
20	58.5	0.32	36.75	10.79	-5	-50.985
30	58.5	0.32	56.37	16.41	-5	-50.985
40	58.5	0.32	73.09	21.13	-4	-40.788
50	58.5	0.32	89.91	25.95	-3	-30.591
60	58.5	0.32	110.10	31.17	-3	-30.591
70	58.5	0.32	117.88	34.74	-2	-20.394
80	58.5	0.32	152.11	43.38	-1	-10.197
90	58.5	0.32	147.47	42.57	-1	-10.197
100	58.5	0.32	154.81	42.14	-0.5	-5.0985
120	58.5	0.32	159.96	41.37	0	0
150	58.5	0.32	163.09	44.15	0	0
200	58.5	0.32	168.41	44.13	0	0

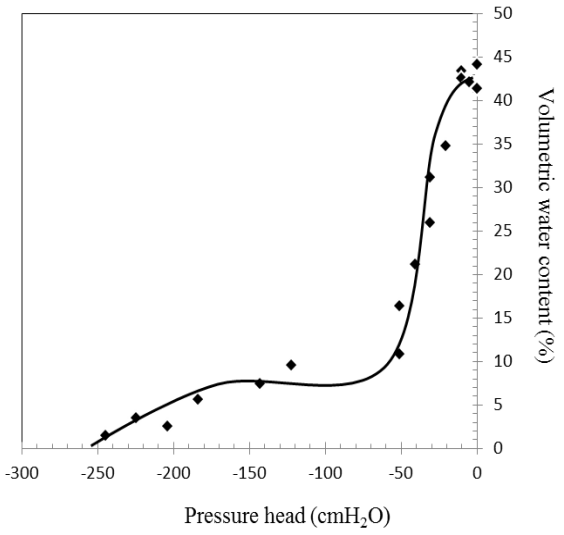

Figure B.3 Water retention curve of silt

van Genuchten model applied to the data observed in the soil column. The soil water retention curve is given in Figure B.4. The saturated volumetric water content; θ_s is 0.441 and residual moisture content; θ_r is 0.014. The volumetric moisture content at *P*; θ_p is 0.208, and the slope; *S* is 0.223. The S_p is 0.507. $Log(h_b)$ is 2.5 The coefficients of *m*, *p* and *a* are 0.180, 1.040 and 0.052, respectively.

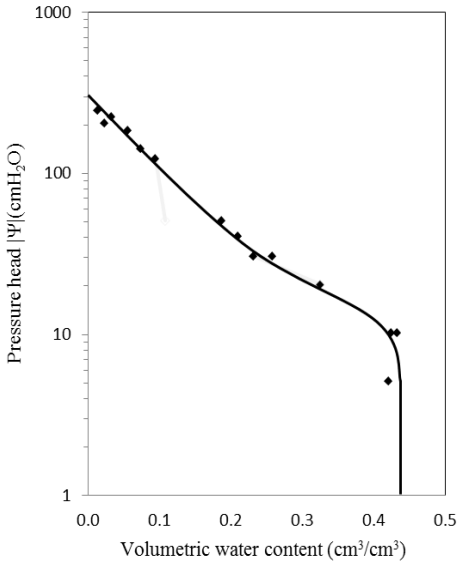

Figure B.4 Sand water retention curve

APPENDIX C

Hydraulic pressured head distribution

Table C.1 Hydraulic pressured head in sand layer in different climate conditions

Elevation of tensiometer (cm)	**hydraulic pressured head (centibar)**		
	drought with stationary sea level	**drought with sea level rise**	**flood with stationary sea level**
(Top) 20	-11	-11	0
18	-11	-11	-1
15	-11	-11	-1.5
12	-10	-10	-2
9	-9	-9	-2
6	-6	-4	-1.5
3	-3	-2	-1
(Bottom) 0	-1	-1	0

Table C.2 Hydraulic pressured head in silt layer in different climate conditions

Elevation of tensiometer (cm)	**hydraulic pressured head (centibar)**		
	drought with stationary sea level	**drought with sea level rise**	**flood with stationary sea level**
(Top) 20	-22	-22	0
18	-18	-18	-0.5
15	-14	-15	-1
12	-12	-11	-2
9	-6	-8	-2
6	-4	-4	-1
3	-2	-2	0
(Bottom) 0	-1	0	0

APPENDIX D

Volumetric water content distribution

Table D.1 Volumetric water content in sand layer in different climate conditions

Elevation of cutting (cm)	**Volumetric water content (cm^3/cm^3)**		
	drought with stationary sea level	**drought with sea level rise**	**flood with stationary sea level**
(Top) 18	0.34	0.34	0.40
15	0.35	0.33	0.36
12	0.38	0.37	0.33
9	0.39	0.39	0.32
6	0.40	0.40	0.33
3	0.41	0.40	0.38
(Bottom) 0	0.41	0.41	0.41

Table D.2 Volumetric water content in silt layer in different climate conditions

Elevation of cutting (cm)	**Volumetric water content (cm^3/cm^3)**		
	drought with stationary sea level	**drought with sea level rise**	**flood with stationary sea level**
(Top) 18	0.02	0.03	0.46
15	0.03	0.05	0.36
12	0.15	0.09	0.3
9	0.21	0.25	0.34
6	0.25	0.40	0.40
3	0.44	0.46	0.44
(Bottom) 0	0.46	0.44	0.46

APPENDIX E

Concentration profile of NaCl in unsaturated porous media

Table E.1 Concentration of NaCl in sand layer different climate conditions

Elevation of cutting (cm)	Concentration of NaCl					
	drought with stationary sea level		drought with sea level rise		flood with stationary sea level	
	EC 1:5 (ms/cm)	Concentration (g/L)	EC 1:5 (ms/cm)	Concentration (g/L)	EC 1:5 (ms/cm)	Concentration (g/L)
(Top) 20	1.98	14.69	2.65	19.66	0.00	0.00
18	2.36	17.51	2.19	16.25	0.00	0.03
16	2.06	15.28	2.25	16.69	0.00	0.02
14	2.29	16.99	2.13	15.80	0.10	0.71
12	2.54	18.84	2.48	18.40	1.35	10.01
10	2.56	18.99	2.46	18.25	1.66	12.31
8	2.57	19.07	2.63	19.51	1.45	10.76
6	2.63	19.51	2.59	19.21	2.02	14.99
4	2.61	19.36	2.64	19.58	1.92	14.24
2	2.59	19.21	2.69	19.96	3.03	22.48
(Bottom) 0	55.45	35.00	55.45	35.00	55.45	35.00

Table E.2 Concentration of NaCl in silt layer in different climate conditions

Elevation of cutting (cm)	Concentration of NaCl					
	drought with stationary sea level		drought with sea level rise		flood with stationary sea level	
	EC 1:5 (ms/cm)	Concentration (g/L)	EC 1:5 (ms/cm)	Concentration (g/L)	EC 1:5 (ms/cm)	Concentration (g/L)
(Top) 20	3.66	1.5	3.66	1.5	0.01	0.04
18	3.66	1.5	3.66	1.5	0.02	0.07
16	3.66	1.5	3.66	1.5	0.04	0.14
14	3.66	1.5	3.66	1.5	0.06	0.21
12	3.66	1.5	3.66	1.5	0.26	0.93
10	5.11	18.20	5.22	18.59	0.18	0.64
8	4.85	17.27	5.01	17.84	0.32	1.14
6	5.08	18.09	4.90	17.45	0.67	2.39
4	4.96	17.66	5.16	18.37	0.51	1.82
2	5.11	18.20	5.22	18.59	0.24	0.85
(Bottom) 0	55.45	35.00	55.45	35.00	55.45	35.00

CURRICULUM VITAE

NAME Mr. Nattachat Boonchukusol

DATE OF BIRTH 21 July 1987

EDUCATIONAL RECORD

HIGH SCOOL
High School Graduation
Sisaket Wittayalai School, 2007

BACHELOR'S DEGREE
Bachelor of Engineering
(Environmental Engineering)
Suranaree University of Technology, 2010

MASTER'S DEGREE
Master of Engineering
(Environmental Engineering)
King Mongkut's University of Technology
Thonburi, 2012

PUBLICATIONS

Nattachat, B. and Bunsri, T., 2013 "Model for Estimating of Salt Intrusion under Changing of Climatic Condition" **2nd International Conference on Environmental Science & Engineering and Management**, March 27-29, 2013 at Pullman Khon Kaen Raja Orchid, Thailand

Nattachat, B. and Bunsri, T., 2013 "Modelling of Salt Intrusion under Heavy Rainfall Infiltration" **International Conference Environmental and Hazardous Substance Management towards a Green Economy**, May 21-23, 2013 at Imperial Queen's Park Hotel, Bankok, Thailand